Fragility of the mean-field scenario of structural glasses for disordered spin models in finite dimensions

Chiara Cammarota,[1,2,*] Giulio Biroli,[1,†] Marco Tarzia,[2,‡] and Gilles Tarjus[2,§]

[1]*IPhT, CEA/DSM-CNRS/URA 2306, CEA Saclay, F-91191 Gif-sur-Yvette Cedex, France*

[2]*LPTMC, CNRS-UMR 7600, Université Pierre et Marie Curie, boîte 121, 4 Pl. Jussieu, 75252 Paris cédex 05, France*

(Received 11 October 2012; revised manuscript received 18 January 2013; published 21 February 2013)

At the mean-field level, on fully connected lattices, several disordered spin models have been shown to belong to the universality class of "structural glasses" with a "random first-order transition" (RFOT) characterized by a discontinuous jump of the order parameter and no latent heat. However, their behavior in finite dimensions is often drastically different, displaying either no glassiness at all or a conventional spin-glass transition. We clarify the physical reasons for this phenomenon and stress the unusual fragility of the RFOT to *short-range* fluctuations, associated, e.g., with the mere existence of a finite number of neighbors. Accordingly, the solution of fully connected models is only predictive in very high dimension, whereas despite being also mean-field in character, the Bethe approximation provides valuable information on the behavior of finite-dimensional systems. We suggest that before embarking on a full blown account of fluctuations on all scales through computer simulation or renormalization-group approach, models for structural glasses should first be tested for the effect of short-range fluctuations and we discuss ways to do it. Our results indicate that disordered spin models do not appear to pass the test and are therefore questionable models for investigating the glass transition in three dimensions. This also highlights how nontrivial is the first step of deriving an effective theory for the RFOT phenomenology from a rigorous integration over the short-range fluctuations.

DOI: 10.1103/PhysRevB.87.064202 PACS number(s): 64.70.Q−, 75.10.Nr, 64.70.pm

I. INTRODUCTION

The random first-order transition (RFOT) theory[1,2] of the glass transition builds on a mean-field scenario in which a complex free-energy landscape with an exponentially large number of metastable states emerges below a critical temperature T_d and the configurational entropy associated with these metastable states vanishes at a lower temperature T_K. At T_K, an RFOT, i.e., a transition with a discontinuous order parameter yet no latent heat, to an ideal glass takes place. This scenario is realized in mean-field-like approximations of a variety of glass-forming systems (liquid models, lattice glasses, uniformly frustrated systems) as well as in mean-field, fully connected, spin models with quenched disorder[2,3] (e.g., p-spin model, Potts glass). The latter correspond to spin glasses without spin inversion symmetry, and their behavior differs from that of the fully connected Sherrington-Kirkpatrick Ising spin glass, which is characterized by a continuous transition in place of the RFOT. They have been investigated in great detail and have provided most of the clues about the generic behavior of "mean-field structural glasses."

To make progress toward a theory of the glass transition, one must, however, go beyond the mean-field description and include the effect of fluctuations[4] in finite-dimensional systems with finite-range interactions. The main assumption behind the RFOT theory of glass formation is that the mean-field scenario with a dynamic and a static critical temperature retains some validity when fluctuations are taken into account. The ergodicity breaking transition at T_d is expected to be smeared and the metastable states no longer have an infinite lifetime because of entropically driven nucleation events. This underlies the picture of a glass-forming liquid as a "mosaic state" with its relaxation to equilibrium dominated by thermally activated rare events involving "entropic droplets."[1] Yet, the main ingredients associated with the RFOT are assumed to persist, even if renormalized by the effect of the fluctuations.[2] The issue can be understood in the much simpler setting of the liquid-gas transition of simple fluids. The mean-field van der Waals approach predicts a liquid-gas transition with a terminal critical point. It is known that this homogeneous mean-field picture needs to be modified, e.g., through the classical nucleation theory and the renormalization group: concepts such as metastability and spinodal are no longer crisply defined, critical exponents as well as nonuniversal quantities are modified, yet the transition with the two, liquid and gas, free-energy states remains valid, at least when the dimension d is larger than 1. In $d = 1$, the mean-field treatment is plain wrong and predicts a transition that is not present. Fluctuations can therefore have a more or less dramatic influence on the mean-field scenario: this is the key-point concerning the relevance of the RFOT theory to glass-forming liquids.

One natural path to follow in order to investigate the effect of the fluctuations on the RFOT and the two-temperature picture is then to consider, both numerically and analytically, the various proposed models of structural glasses in finite dimensions. The disordered spin models are especially convenient as they are both well defined at the mean-field level and much easier to investigate than more realistic models of structural glass-formers or effective Ginzburg-Landau theories in the replica formalism. In particular, they quite directly lend themselves to computer simulations and to real-space renormalization group (RG) treatments. The major obstacle on this seemingly straightforward route is that so far no traces of the RFOT scenario have been found in such studies on finite-dimensional, finite-range models, with either a complete absence of transition to a glass phase[5] or a behavior more compatible with a continuous spin-glass transition[6] than a discontinuous "random first-order" one.

In this work, we clarify the reasons for the discrepancy between the solution of mean-field fully connected disordered spin models and their finite-dimensional behavior. All fully connected models that we have studied (Potts glasses, M-p-spin models and generalizations) provide predictions that turn out to be correct in very high dimensions only: because of their infinite connectivity, they indeed neglect local fluctuations and strongly enhance frustration compared to their finite-dimensional counterpart.

This stresses the importance of considering the implications and the effects of *local, short-range* fluctuations on the existence of the RFOT. If one envisages integrating out the effect of the fluctuations in a renormalization group setting, it is often possible to proceed in a stepwise manner. First, one includes the short-range fluctuations up to a given scale and derives in this way an effective theory that describes the physics on longer distances (or lower energies). The next stage is then to solve the effective theory by accounting for the *long-range* fluctuations, a usually highly nontrivial task. In the study of critical phenomena and phase transitions, the first step is, in general, bypassed and one relies instead on an effective Ginzburg-Landau model based on general symmetry arguments or on the mean-field solution of the microscopic model to which gradient terms are added in order to allow for spatial fluctuations. Generically, the type of mean-field theory considered does not matter. However, it *does* matter in all of the disordered spin models that we have studied. As we shall show, the solution on fully connected lattices or in infinite dimension is not representative of the situation in finite-dimensional systems because it misses the effect of the (purely) short-range fluctuations associated with the mere existence of a limited number of neighbors. On the other hand, a better account of the latter is provided by the Bethe approximation, which, despite being mean-field in character, properly describes the local effect of a finite connectivity. The case of the Potts glass, which we shall discuss in detail, is paradigmatic. In their computer simulation study, Brangian *et al*.[5] found no transition and no glassy behavior for a ten-state Potts glass model in three dimensions, contrary to what was obtained in infinite dimensions. We show here that this is actually expected on physical grounds and confirm this through the solution of the model within the Bethe approximation.

The outcome of our study is twofold: (1) stressing the importance to test the influence of short-range fluctuations on models of structural glasses through the Bethe approximation or similar approaches and (2) showing that disordered spin models mostly appear to fail the test and are therefore questionable starting points for investigating the glass transition in three dimension. We should however add a caution note: we have only considered disordered models in which spins are coupled on pairs of nearest neighbor sites (on a lattice); models with interactions that irreducibly couple degrees of freedom on more than two sites deserve further investigation.

II. FROM INFINITE TO FINITE DIMENSION: DIFFICULTIES AND PUZZLES

On the way to finding a RFOT in finite-dimensional disordered spin models, several difficulties have been identified. (1) The RFOT can give way to a continuous transition to a spin glass, with a quite different phenomenology. This phenomenon was observed for several models when studied by numerical simulations in finite dimensions, see, e.g., Ref. 6. The lack of evidence for the entropy crisis predicted by the RFOT theory in finite-dimensional disordered spin models has been rationalized by invoking the fact that, already at the mean-field level, the relative temperature interval between T_d and T_K is very small for "reasonable values" of the number p of irreducibly interacting spins in the p-spin glass model or of the number q of states in the Potts glass model (say, $p,q \lesssim 10$); under such conditions, the phenomenology should then look more like that of a standard Ising spin glass than that coming with an RFOT. Eastwood and Wolynes[7] have related this to the small value of the reduced surface tension between glassy states in such models and argued that the p's and q's that would be necessary to mimic structural glasses to be $p \simeq 20$ and $q \simeq 1000$.

(2) The RFOT to an ideal glass can be superseded by a conventional (usually ferromagnetic) ordering transition. This phenomenon takes place, for instance, in the disordered Potts models where a tendency to a simple nonglassy ferromagnetic order was observed. Actually, this is also what happens in more realistic models of supercooled liquids in which there is always a transition to the crystal. In the latter case, however, since the transition is first-order one can supercool the liquid and study the metastable glassy phase. This in turn is impossible if the glass transition is superseded by a second-order phase transition, as the above mentioned ferromagnetic one.

Either as a result of the above difficulties or in trying to avoid them, it is often found that no remnants of the RFOT are present in finite dimensions. Actually, it may also be that no transitions at all are observed if one has succeeded in getting around points (1) and (2). An example is provided by the model studied by Brangian *et al*.[5] These authors considered a disordered Potts glass with a distribution of couplings that is displaced toward the antiferromagnetic ones, and that, as a result, has only a small fraction of ferromagnetic couplings. This is a general procedure to avoid ferromagnetic ordering in models without spin-inversion symmetry. (An alternative suggestion is to study an all-ferromagnetic or all-antiferromagnetic Potts model with random permutations of the q states; the latter enforce a statistical gauge symmetry that prevents ferromagnetic or antiferromagnetic ordering.)[8–10] In practice, Brangian *et al*. focused on a ten-state Potts glass model with a bimodal distribution of the couplings having only a fraction $x \simeq 15\%$ of ferromagnetic (positive) ones. Their main result, which is often cited as a major problem for the RFOT theory, is that the three-dimensional model is not glassy at all despite the fact that the mean-field solution in infinite dimension predicts a strong RFOT transition for such a large number of states. This and further analytical and numerical work led for instance Moore *et al*.[11] to put forward the drastic proposal that the RFOT never survives in three dimensions, its phenomenology being instead replaced by that of a conventional spin glass in a magnetic field (which has no transition in three dimensions according to the droplet theory).[12,13]

In the following, we investigate the robustness of the RFOT in spin models with quenched disorder that display such a transition in their mean-field fully connected limit. We clarify how the above listed difficulties arise when lowering the dimension from infinity down to three. We restrict ourselves to

systems with short-range interactions involving only pairs of nearest-neighbor sites on a lattice. This choice is motivated by the fact that such models are amenable to real-space RG analyses and that they are easier to study numerically in comparison to systems where multisite interactions are present, such as the p-spin model. We first focus on Potts glasses and show that by trying to avoid problems (1) and (2), one actually imposes contradictory requirements in finite dimensions; when the distribution of couplings is mostly antiferromagnetic, spontaneous ferromagnetic ordering is indeed thwarted, but considering large values of the number of states q then suppresses frustration and leads to no glass transition at all. We then analyze two alternative types of models: the M-p-spin models introduced in Ref. 14 and a new class introduced by us. We discuss the physical reasons that make the predictions based on the solution of the infinite-dimensional model inadequate in low dimensions, pointing out, as already mentioned, the importance of short-range fluctuations.

III. DISORDERED POTTS MODELS

This section is devoted to a systematic study of disordered Potts models on lattices with finite connectivity. Our aim is to understand the physical reasons that make the discontinuous glass transition (RFOT) so elusive for these systems. We shall show that the two conflicting requirements discussed above actually put severe constraints on the dimensionality and the connectivity of the possible lattices.

A. Models

We define in the following the two Potts models that we shall focus on.

(1) Potts glass with q states. Its Hamiltonian is given by

$$H = -q \sum_{\langle i,j \rangle} J_{ij}\, \delta_{\sigma_i \sigma_j}, \tag{1}$$

where the coupling constants J_{ij} are quenched random variables, and the σ_i's are N Potts variables that can take q different values, $\{1,2,\ldots,q\}$. The symbol $\langle i,j \rangle$ means that each pair of nearest-neighbor sites i,j on the lattice is included in the sum only once and $\delta_{\sigma\sigma'}$ is the Kronecker symbol. We consider bimodal and Gaussian distributions of the coupling constants. The mean-field solution of this model was worked out in Ref. 15 and depends only on the mean and the variance of the coupling constant distribution, denoted J_0 and $(\Delta J)^2$, respectively. By scaling J_0 and $(\Delta J)^2$ with the spatial dimension d as

$$J_0 = \frac{\hat{J}_0}{d}, \quad (\Delta J)^2 = \frac{1}{2d}, \tag{2}$$

where, for convenience, we use the rescaled ΔJ as the unit of energy and temperature, one obtains a well-defined mean-field model in the limit $d \to \infty$. (The same is true in the limit $N \to \infty$ when considering a completely connected lattice and replacing d with the number of sites N.)

A detailed presentation of this model is postponed to the following section. Here, we just recall the main result obtained within mean-field theory. Note that we only focus on the case $q > 4$. This corresponds to models displaying a dynamical ergodicity-breaking transition at a temperature T_d and a RFOT at a temperature T_K. The former is in the class of the singularity found in the mode-coupling theory of liquids and the latter is akin to an entropy-vanishing, Kauzmann-like, discontinuous glass transition. Lower values of q lead to a continuous spin-glass transition.[6] As discussed before, it is important to take $\hat{J}_0$ negative enough in order to avoid ferromagnetic ordering. In practice, this means $\hat{J}_0 < -\frac{p-4}{2}\frac{1}{2T}$. The dynamical and static transition temperatures depend on q as $T_d \sim \sqrt{\frac{q}{2\ln q}}$ and $T_K \sim \frac{1}{2}\sqrt{\frac{q}{\ln q}}$ for $q \gg 1$.[16] The values of the jump in the (overlap or spin-glass) order parameter at T_d and T_K both tend to one in the large q limit, indicating that the larger the number of states the more discontinuous the transition at T_K.

(2) Random-permutation Potts magnet. Its Hamiltonian reads

$$H = J \sum_{\langle i,j \rangle} \delta_{\sigma_i, \pi_{ij}(\sigma_j)}, \tag{3}$$

where $J > 0$ (antiferromagnet) or $J < 0$ (ferromagnet) and π_{ij} is a random permutation of the q colors that is attached to the edge between i and j.[17] This model has a "gauge invariance" that prevents antiferromagnetic or ferromagnetic ordering;[8–10] indeed, if one permutes the states of the spin at a given site i, one can always find random permutations associated with all edges emanating from i such that the energy does not change; after averaging over the quenched disorder (i.e., random permutations), the (staggered) magnetization is then zero. This model has been studied by numerical simulation[9] in its ferromagnetic version and by the cavity method[10] in its antiferromagnetic version. In the latter case, the $T = 0$ limit describes a form of "coloring problem," the states being then interpreted as colors.

B. Frustration and lack thereof for $q \gg 1$

In the search for finite-dimensional models displaying glassy phenomenology, the disordered Potts models have played a central role. They were actually at the root of the RFOT theory of the glass transition in the pioneering papers by Kirkpatrick, Thirumalai, and Wolynes.[1] For this reason and also because the mean-field studies cited above predicted a strong discontinuous glass transition for a large number of states (or colors), they seemed to be the most promising candidates to find a RFOT in three dimensions. It thus came as a surprise that simulation results[5] instead showed a complete absence of glassy phase for a $q = 10$ disordered Potts model.

Our claim, which we substantiate in the following, is that the original intuition based on the infinite-dimensional limit (or the study of fully connected lattices) is misguided. A first piece of explanation comes by considering the degree of frustration, which is known to be central for the existence of glassy phases. This is most clearly understood in the case of the disordered antiferromagnetic Potts model, which corresponds to a coloring problem at zero temperature. For any *finite-connectivity* lattice, such a model becomes unfrustrated for q large enough: in physical terms, if the number of states, i.e., colors, is too large for a given coordination number then it becomes easy to arrange them in a way that two neighboring sites do not have the same color, hence lifting frustration. Therefore one does

not expect any glassy phase for large q on a finite- connectivity and, in particular, a finite-dimensional lattice.

The recent study of the antiferromagnetic Potts model with random color permutations on (both regular and Erdös-Rényi) random graphs of finite coordination number c (see Ref. 10) supports our claim. It was shown that the model for $q \geqslant 4$ may have a phenomenology similar to that of other mean-field structural glasses, with a RFOT accompanied by a dynamical transition at T_d. However, in agreement with our previous discussion, the RFOT disappears at fixed coordination number c when the number of colors q is sufficiently large; for instance, for $c \leqslant 8$ the transition disappears already at $q = 4$, and for $c \leqslant 13$ there is no phase transition at $q = 5$. Asymptotically, the transition is absent when $2q \ln(q) - \ln(q) - 2\ln(2) > c$ (see a footnote in Ref. 18). For a given lattice coordination number, frustration, hence glassy phenomenology, is therefore lost when q is too large, typically larger than $(c/2)/\ln(c/2)$.

The same trend takes place in Euclidean lattices. We indeed prove in Appendix A that the q-state antiferromagnetic Potts model with random color permutations has no phase transition on Euclidean lattices when $q > 2c$. This generalizes a proof by Salas and Sokal[19] that applies to the standard random antiferromagnet Potts model. In particular, we show that there is a unique infinite-volume Gibbs measure with exponential decay of the correlations at all temperatures and for any realization of the random permutations. Quite generally then, frustration vanishes for a large number of colors or states, as intuitively expected.

C. Bethe approximation of the ten-state three-dimensional Potts glass model

In the previous section, we have shown that frustration vanishes when the number of states q becomes sufficiently large at fixed coordination number in random antiferromagnetic Potts models on both Euclidean lattices and random graphs. As a result, any putative glassy phase transition is wiped out. We now study the effect of adding a fraction of ferromagnetic couplings. This should introduce frustration and possibly lead to RFOT phenomenology. We shall see, however, that this is not the case.

In the following, we focus on the model considered by Brangian *et al.*,[5] which we have investigated through the Bethe approximation; in practice, we have then studied the $q = 10$ Potts glass on a random graph with the same coordination number as the cubic lattice, $c = 6$. We have used the cavity method that allows for an analytic solution. The main steps of our calculations are illustrated in Appendix B. Potts glasses (with a different coupling distribution) were already studied in Ref. 10, where the general cavity approach for Potts glasses is also discussed. In the following, we only report the main results.

In this model, the distribution of the couplings is bimodal,

$$P(J_{ij}) = x\delta(J_{ij} - J) + (1 - x)\delta(J_{ij} + J), \qquad (4)$$

where $J = \sqrt{2}$ and the fraction of ferromagnetic couplings x varies from 0 to 1. The value considered by Brangian *et al.* is $x = (2 - \sqrt{2})/4 \simeq 0.146$.[5] The phase diagram that we have obtained within the Bethe approximation is reported in Fig. 1.

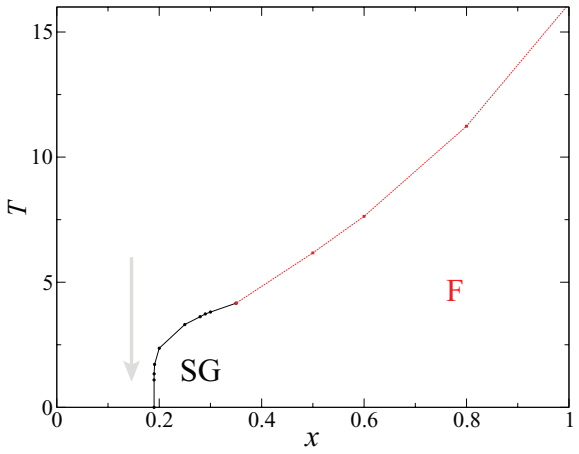

FIG. 1. (Color online) Phase diagram of the ten-state three-dimensional Potts glass with bimodal disorder predicted by the Bethe approximation. The value of x shown by the arrow corresponds to that studied by Brangian *et al.*[5] The black circles correspond to the transition between the paramagnetic and the spin-glass phases where the spin-glass susceptibility diverges. The red squares correspond to the first-order transition between the paramagnetic and the ferromagnetic phases where the free energies of the two phases cross. There is also a transition line between the ferromagnetic and the spin-glass states, which we do not report. The uncertainty due to the numerical solution of the cavity equations is smaller than the size of the points (see Appendix B for a discussion). The line connecting the points are guides for the eye.

There is no discontinuous glass transition (RFOT) for any positive fraction x of ferromagnetic couplings. Instead, for relatively small values of x, we find a continuous spin-glass transition, and above some threshold, this spin-glass transition is superseded by a ferromagnetic one. The model is not glassy at all for $x = (2 - \sqrt{2})/4 \simeq 0.146$, at any temperature. Although there is no general proof, one expects that frustration on Euclidean lattices is comparable or less than that found on random graphs. Thus the absence of a RFOT on a random graph for $x = (2 - \sqrt{2})/4 \simeq 0.146$ is fully compatible with the numerical results of Brangian *et al.*

From this analysis, we therefore conclude that adding a small fraction of positive couplings is not sufficient to trigger the appearance of a discontinuous glass transition when the connectivity is finite and the number of states large. In addition, this shows that the absence of RFOT in the three-dimensional model studied by Brangian *et al.* is not primarily due to some long-distance, possibly, nonperturbative fluctuations but is just a consequence of the local property of the lattice, namely, the fact that the connectivity is too small compared to the number of colors. This effect is correctly captured by the Bethe approximation. It is instead completely missed by the mean-field analysis based on a fully connected lattice, which therefore appears to be quite misleading to predict the behavior of three-dimensional systems.

An additional question that could provide a valuable hint for future studies concerns the smallest value of the spatial dimension d (and of the associated number of states q) such that Potts disordered models show a discontinuous glass transition (RFOT) within the Bethe approximation. We

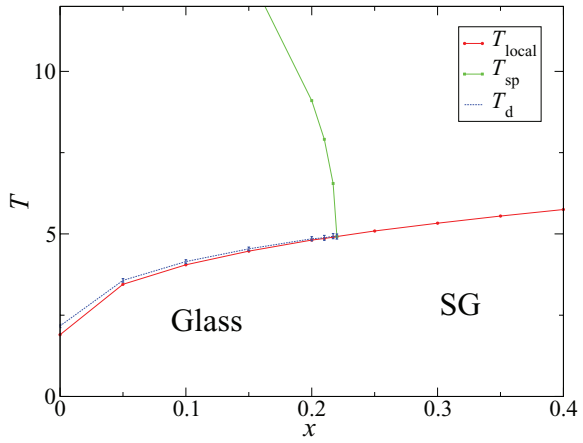

FIG. 2. (Color online) Phase diagram of the five-state Potts glass with bimodal disorder on a regular random graph of coordination number $c = 18$ as a function of x and T, showing $T_{\rm sp}$ (green squares) where the paramagnetic phase becomes unstable towards the antiferromagnetic order, $T_{\rm local}$ (red circles) where the RS solution becomes unstable towards RSB, and the dynamical temperature T_d (blue points). The numerical uncertainty on $T_{\rm sp}$ and $T_{\rm local}$ is smaller than the symbols' size. The error bars indicate the uncertainty on T_d due to numerical procedure (see Appendix B for a discussion). The line connecting the points are guides for the eye. We do not know if the virtual coincidence of the points at which $T_{\rm local}$ merges with T_d on the one hand and with $T_{\rm sp}$ on the other is a result of the numerical uncertainty (that we cannot exclude, see the error bars) or has a deeper significance.

consider as a prototypical example the case of the Potts model with the distribution of the couplings given by Eq. (4) with $q = 5$ states and placed on a regular random graph of coordination number $c = 18$ (which would mimic a hypercubic lattice in nine dimensions).

The phase diagram of the model, which we have obtained through the cavity method, is shown in Fig. 2 as a function of x and T. For a small enough x ($x \leqslant 0.22$), where most of the couplings are antiferromagnetic, there is enough frustration to produce a RFOT, as previously shown for $x = 0$.[10] This is demonstrated by the fact that the dynamical critical temperature T_d is higher than the temperature $T_{\rm local}$ at which the replica-symmetric (RS) solution becomes unstable towards replica-symmetry breaking (RSB). However, the glass transition is superseded by an antiferromagnetic transition, which takes place at a much higher temperature. We have computed the temperature $T_{\rm sp}$ at which the paramagnetic solution becomes unstable towards antiferromagnetic order,[20] see Fig. 2. This transition will likely be very difficult to avoid in any numerical simulation on Euclidean lattices, unless random permutation of colors is considered. As the value of x is increased, $T_{\rm sp}$ decreases, but, at the same time, the distance between $T_{\rm local}$ and T_d reduces, and the glass transition becomes less and less discontinuous. Finally, when $x > 0.22$, where there is no instability towards the antiferromagnetic order, the glass transition becomes continuous and a conventional spin-glass phase is found.

This example confirms that even in a dimension as high as $d = 9$, avoiding the two problems listed in Sec. II imposes conflicting constraints that are very hard to fulfill. Some improvement could come from considering random permutations in order to avoid the appearance of an antiferromagnetic phase. Even in this case, one would have to consider for $q = 4$ at least $c \geqslant 12$, i.e., $d \geqslant 6$ for a hypercubic lattice.

IV. THE APPROACH TO THE INFINITE-DIMENSIONAL OR FULLY CONNECTED LIMIT

In this section, we study the $1/d$ expansion for the q-state Potts glass on Euclidean hypercubic lattices of coordination number $c = 2d$. The aim of this analysis is to better understand the regime of validity of the mean-field results, which, as found in the previous section, appears to be rather limited.

We have derived the $1/d$ expansion of the replicated Gibbs free energy by following the method developed by Georges, Mézard, and Yedidia.[21,22] We have focused on a Gaussian distribution of couplings. In order to perform the $1/d$ expansion, it is useful to introduce the simplex representation of the model as follows:

$$H = -\sum_{\langle i,j\rangle} J_{ij} \sum_{a=1}^{q-1} S_{i,a} S_{j,a}. \tag{5}$$

In this representation, q is the number of colors and the degrees of freedom $S_{i,a}$ are vectors pointing toward the q vertices of a tetrahedron in a $(q-1)$-dimensional space.[23] The order parameter within the replica treatment reads

$$Q_i^{\alpha\beta} = \langle S_{i,a}^{\alpha} S_{i,a}^{\beta} \rangle = \langle \delta_{\sigma_i^{\alpha}\sigma_i^{\beta}} \rangle, \tag{6}$$

where α and β are replica indices. We refer to Ref. 23 for more details on the replica theory for Potts glasses. When using the simplex representation, the Hamiltonian of the Potts model is very similar to that of the Edwards-Anderson (Ising) model. The $1/d$ expansion can then be performed through the high-temperature expansion of the replicated Gibbs free energy.[21] In the case of Potts variables the computation is more cumbersome. For this reason, we only consider the first order in $1/d$. The detailed computation is presented in Appendix B and in the following we only report the main results.

The Gibbs free-energy A can be obtained as an expansion in $Q^{\alpha\beta}$. We focus on the first three terms only since this is enough to discuss the existence and the properties of the glass transition:

$$-\beta A \simeq N \Bigg[\sum_{\alpha\neq\beta} -\frac{t}{4} (Q^{\alpha\beta})^2 + \frac{w_1}{6} \mathrm{Tr}(Q^3) + \sum_{\alpha\neq\beta} \frac{w_2}{6} (Q^{\alpha\beta})^3 + \cdots \Bigg]. \tag{7}$$

The coefficients of the expansion computed at the first order in $1/d$ read

$$\begin{aligned} t &= 1 - \beta^2 - \frac{\beta^4}{4d}(q^2 - 10q + 10) \\ &\quad - 2(q-2)\beta^3 \frac{\tilde{J}_0}{d} - 2\frac{(\beta \tilde{J}_0)^2}{d} \\ w_1 &= 1 - \frac{3\beta^4}{2d}(q-1), \qquad w_2 = \frac{q-2}{2}, \end{aligned} \tag{8}$$

where

$$\beta\tilde{J}_0 = \left[\beta\hat{J}_0 + \frac{\beta^2(q-2)}{2}\right]. \tag{9}$$

As in the mean-field solution ($d \to \infty$), we consider a one-step replica symmetry broken (1-RSB) form for $Q^{\alpha\beta}$: the replicas are grouped in n/m groups of m elements and $Q^{\alpha\beta}$ is equal to Q for all pairs belonging to the same group and to zero otherwise. In order to study the glass transition, one has to focus on the $m \to 1$ limit of $(\beta A)/(m-1)$ which, within the 1-RSB ansatz, reads

$$\lim_{m\to 1} \frac{\beta A}{m-1} = \frac{t}{4}Q^2 - \frac{w_2 - w_1}{6}Q^3 + \cdots .$$

Within this formalism, a discontinuous glass transition (i.e., a RFOT) is signaled by the sudden change of the global minimum of $(\beta A)/(m-1)$ from $Q = 0$ to $Q = Q_{\mathrm{EA}} > 0$ (where Q_{EA} is the Edwards-Anderson order parameter). A negative sign of the coefficient of the cubic term, i.e., $w_2 > w_1$, then insures that the transition, if it exists, must be discontinuous. In addition, if the coefficient of the quadratic term, $t/4$, becomes negative below a temperature T_{local}, then a discontinuous transition surely takes place for $T \geqslant T_{\mathrm{local}}$. In the strictly infinite-dimensional limit, one finds $w_2 > w_1$ for $q > 4$ and $T_{\mathrm{local}} = 1$, in agreement with the exact solution of the model.[15] (One also has to consider $\tilde{J}_0$ equal to zero or negative in order to avoid ferromagnetic ordering.) The magnitude of the coefficient of the cubic term increases (i.e., the term becomes more negative) with the number of states. This fact and the exact mean-field solution showing that $Q_{\mathrm{EA}} \to 1$ for $q \to \infty$ led to the belief that the larger the number of states (or colors) the more strongly discontinuous the transition in finite dimension. The $1/d$ corrections also seem to support this conclusion. Indeed, at $T \simeq T_{\mathrm{local}}$, when $d \gg q^2$, which corresponds to the perturbative regime of the $1/d$ expansion, the corrections make $w_2 - w_1$ larger and T_{local} higher when q increases (if $\tilde{J}_0 \leqslant 0$). The latter condition implies that the scaled mean of the couplings $\hat{J}_0$ is negative enough, i.e., the model is antiferromagnetic enough. This is however quite surprising since for a $\hat{J}_0$ that is very negative, the corresponding finite-dimensional model has almost all of the couplings antiferromagnetic. As we have shown in the previous section, increasing the number of Potts states leads to a decrease of frustration for such a system, and eventually a disappearance of RFOT in finite dimensions. The $1/d$ expansion appears instead to predict just the opposite!

The disagreement between the two approaches (the study on random and Euclidean lattices for a large number of states and the $1/d$ expansion) can be traced back to the fact that in the former case, one considers the limit of large number of states at fixed dimension whereas in the latter, the number of dimension tends to infinity at fixed, although large, number of states. These two different ways of taking the limits of large dimension and of large number of states do not seem to commute. For instance, in the limit of large dimensions, the couplings are such that the average value is typically much less than the standard deviation; $\hat{J}_0/d \ll \Delta J = \sqrt{1/d}$ if d is large enough, no matter what is the value of $\hat{J}_0$. In consequence, the starting point of the $1/d$ expansion is such that almost half of the couplings are positive, whereas the other half are negative, a situation quite different from the finite-dimensional one we would like to describe, i.e., a Potts glass in which almost all of the couplings are antiferromagnetic.

In conclusion, the mean-field infinite-dimensional theory appears to be rather singular. It may still be representative of the physics of finite-dimensional Potts glasses, but only for a very large number of dimensions, and certainly not for the three-dimensional case. (As discussed above, we expect that d has to be larger than the square of the number of states in order to be in the perturbative regime related to mean-field theory.) As a consequence, the free energy in Eq. (7) with the coefficients given by Eq. (8) does not provide a correct effective model for the three-dimensional system even when the first $1/d$ corrections are included.

V. ALTERNATIVE MODELS

In the following, we focus on two classes of disordered models, one introduced in Ref. 14 and one tailored by us, which might provide a better alternative to Potts glasses. Unfortunately, as we shall show, the drawbacks of the disordered Potts models discussed above apply, at least partially, to these alternative models too.

A. The M-p-spin model

The M-p-spin models were first introduced in Ref. 14 and later generalized and studied in Refs. 24 and 11. M Ising spins $S_i^{(\alpha)}$, $\alpha = 1,2,\ldots,M$ are present on each site i of a hypercubic lattice. In this work, we consider the $p = 3$ case, whose Hamiltonian is given in terms of products of three spins chosen from the spins in a pair of nearest-neighbor sites:

$$H = -\sum_{\langle ij\rangle}\sum_{\alpha<\beta}^{M}\sum_{\gamma}^{M}\left[J_{ij}^{(\alpha\beta)\gamma}S_i^{(\alpha)}S_i^{(\beta)}S_j^{(\gamma)} + J_{ij}^{\gamma(\alpha\beta)}S_i^{(\gamma)}S_j^{(\alpha)}S_j^{(\beta)}\right]. \tag{10}$$

The couplings are independently distributed quenched Gaussian variables with zero mean and variance ΔJ^2. Note that the interactions involve three spins but only two sites.

The expansion of the Gibbs free energy in terms of $Q^{\alpha\beta}$, analogous to the one described above, was worked out in Ref. 24 for general values of M and p and $d = \infty$. The unique value of M such that $w_2 > w_1$, i.e., leading to a discontinuous glass transition (RFOT), is $M = 3$ for $p = 3$. This model was later studied by Migdal-Kadanoff real-space RG in three dimensions by Yeo and Moore.[11] They concluded that no glass transition is present in finite dimension and that the behavior of the system resembles more that of a model displaying an avoided continuous spin-glass transition. There is still no numerical simulation testing this prediction (work is in progress).[25]

In order to understand the disagreement between the two approaches (infinite-dimensional mean-field and real-space RG in $d = 3$), we have solved the model on a fully connected lattice with the same choice of scaling for the variance as in Ref. 24: $\Delta J^2 = \frac{1}{9N}$ (this is equivalent to take $d = \infty$ and a variance of the coupling scaling as $1/d$). More details are given in Appendix C. We have found that the dynamical MCT-like transition takes place at $T_d \simeq 0.5970$ and that the

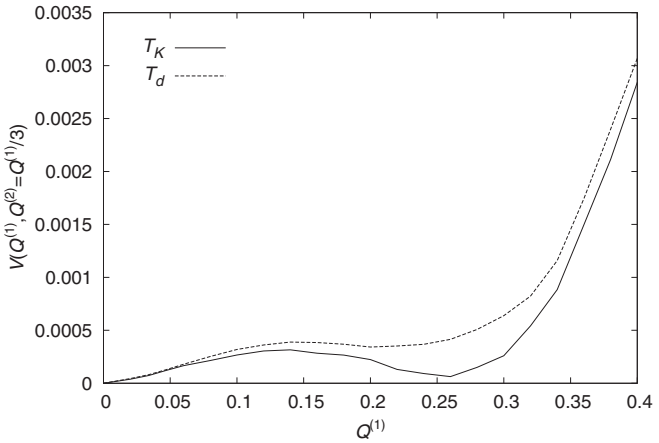

FIG. 3. Plot of $V = (\beta A)/(m-1)$ as a function of the overlap for the M-p disordered model with $M = 3$ and $p = 3$ at T_d (dashed line) and at T_K (continuous line). As discussed in the main text and in Appendix C, the exact solution of the model lead to two kinds of overlaps (or order parameters) $Q^{(1)}$ and $Q^{(2)}$. We plot the Gibbs free energy as a function of $Q^{(1)}$ along the line $Q^{(2)} = Q^{(1)}/3$; a similar behavior is obtained for other choices.

static RFOT takes place at $T_K \simeq 0.5963$. The plot of the Gibbs free energy, $(\beta A)/(m-1)$, within the 1-RSB ansatz is shown in Fig. 3 for $T = T_d$ and $T = T_K$. The most striking fact is the very small value of the free energy for the whole range of overlap. Actually, in the exact solution of the models, two different overlaps emerge: $Q^{(1)} = \sum_i \langle S_i^\alpha \rangle^2/N$ and $Q^{(2)} = \sum_i \langle S_i^\alpha S_i^\beta \rangle^2/N$. We have plotted the free energy along the line $Q^{(2)} = Q^{(1)}/3$ but a similar behavior is obtained for other choices. As we discuss below, the smallness of the free energy is possibly the cause of the lack of robustness of the mean-field results as the finite-dimensional fluctuations not taken into account within mean-field theory are then overwhelming compared to the structure of $(\beta A)/(m-1)$ found in $d = \infty$.

We have not tried to develop a $1/d$ expansion for this model because in finite dimension, due to the lack of inversion symmetry, $S_i \to -S_i$, a nonzero value of the overlap Q_0 (in the 1-RSB scheme) emerges even at high temperature: an amorphous, but trivial, disordered magnetization profile is induced by the quenched disorder. As a consequence, the $1/d$ expansion is more involved (one should make an expansion in $Q - Q_0$).

B. The F model

We now consider another class of models, which is new and presented for the first time in this work. As the previous one, it is characterized by spins with nearest-neighbor interactions. The partition function of the model is defined as

$$Z = \sum_{\{S_i\}} \prod_i \mu\left(S_i^1, S_i^2, S_i^3\right) \exp(-\beta H),$$

where the spins can take the values $-1,0,+1$ and μ gives different weights to the 3^3 states per site; μ is a kind of generalized fugacity. We focus on the case where the only allowed states are $\{1,1,1\}, \{1,-1,-1\}, \{-1,-1,1\}, \{-1,1,-1\}$ and $\{0,0,0\}$, i.e., $\mu = 0$ for all other states. Moreover, we introduce P as the ratio between $\mu(1,1,1)$ and $\mu(0,0,0)$ and we assume that the first four allowed states are all characterized by the same value of μ. (We have considered other variants which have all led to similar results; thus we just present the simplest one.)

The Hamiltonian of the model reads

$$H = -\sum_{\langle i,j \rangle} \sum_a J_{ij}^a S_i^a S_j^a,$$

where the J_{ij}^a's are independently distributed Gaussian random variables with zero mean and variance ΔJ^2. A welcome characteristic of this model is that it has a kind of spin-inversion symmetry, if one flips, say, all S_i^1, S_i^2 the probability measure is invariant (likewise for S_i^1, S_i^3 and S_i^2, S_i^3). In consequence, the average magnetization is zero at high temperature, i.e., Q_0 is equal to zero.

As for the previous model, we have first obtained the development in powers of $Q^{\alpha\beta}$ of the Gibbs free energy for the completely connected model, corresponding to $d = \infty$, by using the scaling $\Delta J^2 = 1/N$:

$$-\beta A \simeq N \left[\sum_{\alpha \neq \beta} -\frac{3t}{4} (Q^{\alpha\beta})^2 + \frac{w_1}{2} \mathrm{Tr}(Q^3) + \sum_{\alpha \neq \beta} \frac{w_2}{2} (Q^{\alpha\beta})^3 + \cdots \right], \tag{11}$$

where $\langle S_i^{a,\alpha} S_i^{a,\beta} \rangle = Q^{\alpha\beta}$ independently of a, i.e., the symmetry between the spins is not broken. The coefficients of the expansion are equal to

$$t = 1 - \beta^2 \langle (S_1)^2 \rangle, \quad w_1 = \langle (S_1)^2 \rangle^3, \quad w_2 = \langle S_1 S_2 S_3 \rangle^2,$$

where $\langle (S_1)^2 \rangle$ and $\langle S_1 S_2 S_3 \rangle$ are on-site spin-spin correlation functions that can be easily computed, see Appendix D. Because of the property of the probability measure μ that we have chosen, it is easy to show that $\langle (S_1)^2 \rangle = \langle S_1 S_2 S_3 \rangle$. Then, by using that $\langle (S_1)^2 \rangle < 1$ (the equality only applies to the $P = 1$ case that we disregard), we obtain that $w_2 > w_1$. In consequence, this model, as the previous ones, undergoes a discontinuous glass transition (RFOT) at a temperature higher than T_{local} (always defined as the temperature at which the coefficient t becomes negative).

We have also worked out the complete mean-field solution of the model and found that if P is too small the glass transition is pre-empted by a standard first-order transition from the high-temperature paramagnetic (liquid) state directly to the amorphous glass state. For values of P larger than $P \simeq 0.035$ the model displays a RFOT, which becomes less discontinuous as P is increased (the barrier at the transition decreases). For instance, for $P = 0.05$, we find $T_d \simeq 0.6608$ and $T_K \simeq 0.6607$ and $Q(T_K) \simeq 0.073$. As found for the M-p-model, the Gibbs free energy is very small for the whole range of overlap Q between the first and the second minimum: see Fig. 4. This feature is observed for any choice of P and for all variants of the weights that we have analyzed. It suggests, as for the M-p-model, that the predictions of the infinite-dimensional mean-field theory remain valid for very high dimensions only.

In addition, we have indeed solved the model on a random graph of connectivity $c = 6$ by using the cavity method. As anticipated, we only find only a continuous spin-glass transition as the temperature is lowered.

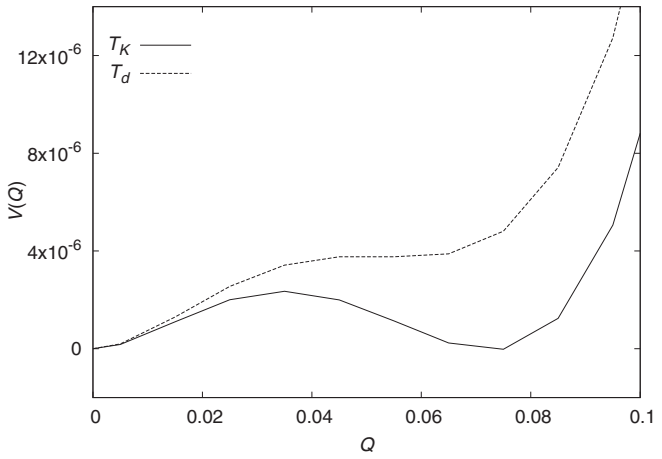

FIG. 4. Plot of $V = (\beta A)/(m-1)$ as a function of the overlap for the F model for $P = 0.05$ at $T_d \simeq 0.6608$ (dashed line) and $T_K \simeq 0.6607$ (continuous line). Note the scale of the free energy.

C. Surface tension and a possible origin for the lack of robustness of infinite-dimensional mean-field glassy phenomenology

In the infinite dimensional versions of the M-p-spin and F-models, we have found that the typical scale of the Gibbs free energy between the first and the second minimum is very small, much smaller than T_K. In the following, we argue along lines similar to those in Ref. 7 that this makes the mean-field predictions very fragile, except in very high dimensions.

The Gibbs free energy as a function of the overlap is the starting point to compute the so-called "surface tension" Y; the latter is equal to the reduction, per unit area, of the total configurational entropy that is caused by fixing the overlap at the value of the secondary minimum outside a ball of radius R. This quantity plays a crucial role in establishing that the glass transition in finite dimension is associated to a growing length scale, called "point-to-set correlation length," and a growing time scale.[2] Moreover, it is also the starting point for RG analyses of the glass transition.[4,26] Studies performed by using instanton techniques[27,28] have shown that the first nonperturbative corrections to mean-field theory lead to a value of Y equal to $\int_0^{Q_{\rm EA}} dQ\sqrt{\beta A/(m-1)}$. Thus a Gibbs free energy that is very small between the two minima $Q = 0$ and $Q = Q_{\rm EA}$, as we found for the previous models, leads to $Y \ll T_K$. This is problematic because, as it has become clear in recent years, some of the fluctuations not considered within mean-field theory correspond to adding an effective quenched disorder and lead to local fluctuations of the surface tension Y and of the configurational entropy density s_c.[29–31] Actually, this is expected on intuitive grounds: on small length scales, the values of Y and s_c must fluctuate in an amorphous system, especially that envisioned as a "mosaic state."[1] The effective quenched disorder affecting Y on microscopic length scales is expected to be of the order of the typical energy scale, i.e., T_K, since it is due to local microscopic fluctuations. In consequence, on small length scales, the disorder is much larger than the surface tension Y when the latter is much smaller than T_K. In this case, heuristic arguments as well as RG-based ones[26] suggest that the RFOT found within mean-field theory is destroyed. This is similar to what happens for the random-field Ising model in finite dimension if the disorder is too strong compared to the ferromagnetic coupling (which plays the role of the surface tension Y).

The same phenomenon is present in the Potts glass model for a reasonable number (less than ten) of states. Eastwood and Wolynes[7] have argued that one could cure the problem and make the surface tension Y large by considering a large number of states, $q \simeq 1000$, thereby preserving the RFOT in three dimensions. However, this is not a proper resolution as one then encounters another obstacle; as we have previously discussed, one indeed expects that frustration, and as a result glassiness, disappear for large q in three dimensions.

VI. FRAGILITY OF THE RFOT SCENARIO FOR FINITE DIMENSIONAL SYSTEMS AND PROPER EFFECTIVE THEORY

As already stressed, there are two main issues to address in order to understand the effect of fluctuations on the RFOT. (1) Once short-range fluctuations are taken into account, is the resulting effective theory RFOT-like? To be so, the model should favor two phases: one (the liquid) in which replica remain uncorrelated and another (the ideal glass) in which replica are correlated and display a high overlap between typical interreplica configurations (the latter phase being metastable with respect to the former for $T > T_K$). (2) If the answer to the previous question is affirmative, do long-distance and, possibly, nonperturbative fluctuations destroy the transition and alter the scenario developed by mean-field and heuristic arguments or not?

These two issues are *mutatis mutandis* always present in physics but the first one is often of little relevance and easily handled in the field of critical phenomena and phase transitions. This is not so in the present case. We have found in the case of the disordered spin models under study a striking fragility of the RFOT scenario to the effect of short-range fluctuations. Despite the fact that the description obtained from the infinite-dimensional/fully connected limit displays a ubiquitous RFOT, the models instead show in finite dimensions no glassy behavior at all or one that is characteristic of a conventional spin-glass transition. The answer to the above first question is therefore negative for these models. This leads us to propose that a model with a putative RFOT should better be first tested for the effect of short-range fluctuations only, before carrying out a full-blown calculation including fluctuations on all scales either by computer simulation or RG treatment. This makes sense for a schematic model that is itself a caricature of the glass-forming liquids one is aiming at describing. For a realistic glass-forming liquid model, the question is rather whether the RFOT approach has any chance to describe its glassy behavior. The issue is then whether one can arrive, by some reasonably well-defined coarse-graining or RG procedure that integrates the short-range fluctuations, at an effective theory in the expected universality class of the RFOT. We discuss below these two aspects without dwelling too much on the first one, which we have already addressed.

(1) Does a given microscopic schematic model lead to RFOT-like behavior once short range fluctuations are included? Most schematic models showing a RFOT in the

infinite dimensional mean-field limit that have been proposed are formulated in terms of discrete variables on a lattice. We suggest to use the Bethe approximation as a first test of the influence of introducing a finite connectivity in the problem. The Bethe approximation is equivalent to solving the model on random regular graphs. These have the same finite connectivity as the Euclidean lattices that they mimic, but of course not the same behavior at long distance due to the absence of loops on all scales and the essentially treelike structure. Thus, within the Bethe approximation, one is able to take into account at least some short-range fluctuations (one can always improve the results by cluster methods) and as a result get a reasonable description of the local physics. If short-range fluctuations completely change the behavior of a model, one expects the Bethe approximation to be able to capture this effect.

As an example, we mention again the ten-state Potts glass studied by Brangian *et al.*[5] The fact that no glass transition was found in the computer simulation study on the three-dimensional cubic lattice could in retrospect have been predicted from the result of the Bethe approximation, which already shows the disappearance of any RFOT for the same connectivity. The approximation is known to overlook the effect of long-distance fluctuations and is mean-field in character. However, it does have some merit to study the physics at short distance.

(2) Is the replicated Ginzburg-Landau free energy predicting a strong RFOT (at the mean-field level) representative of realistic glass-forming liquid models? The Ginzburg-Landau functional that has been postulated to represent the effective theory of structural glasses[27] is given in a replica formalism by

$$\beta\mathcal{F}[Q] = \int d^d x \left(\sum_{\alpha\neq\beta} \left\{ \frac{1}{2}[\partial Q^{\alpha\beta}(x)]^2 + \frac{t}{2} Q^{\alpha\beta}(x)^2 - \frac{w_2}{6} Q^{\alpha\beta}(x)^3 + \cdots \right\} - \frac{w_1}{6} \mathrm{Tr}[Q(x)^3] \right), \quad (12)$$

where $Q^{\alpha\beta}(x)$ is a local, but coarse-grained, (matrix) order parameter describing the overlap among replicas and the number m of replicas has to be taken to $1, m \to 1^+$, to describe the physics associated with an exponentially large number of metastable states (above the RFOT). At the mean-field level, the glass transition can be made as strongly discontinuous as wanted by increasing $w_2 - w_1$. (On the other hand, the transition becomes that of a conventional spin glass in a magnetic field when $w_2 < w_1$.)

However, besides heuristic arguments about coarse graining[32] and guidance from the infinite-dimensional/fully-connected limit [see, e.g., Eqs. (7) and (11)], there has been no serious derivation of the above functional from a proper renormalization step accounting for the contribution of the local short-range fluctuations in a realistic model of glass-forming liquid. As we have precisely seen above how fragile to the latter fluctuations is the RFOT scenario, in the case of disordered spin models, this step should be a prerequisite to validate the RFOT theory as a starting point for describing the glass transition in real systems. Long-range fluctuations can of course destabilize the RFOT even when starting from the replicated Ginzburg-Landau functional with a strongly discontinuous RFOT at the mean-field level, but matters would be much worse if the RFOT is already wiped out by short-range fluctuations. The latter possibility is advocated by Moore and coworkers[11] who suggest that coarse-graining a glass-forming liquid model leads to a Ginzburg-Landau functional akin to that in Eq. (12), but with $w_2 < w_1$, hence with no RFOT at all.

A possible means to capture short-range fluctuations in liquid models is to consider the system within a cavity with amorphous boundary conditions. This method has recently been proposed[33] and applied[34] to measure the growth of amorphous order in glassy systems. It amounts to studying the thermodynamics of a system constrained to have all particles (or spins) outside a cavity in the same positions (or configuration) as those of a typical equilibrium configuration. By construction, degrees of freedom are then integrated out only up to a length-scale which is the size of the cavity. Provided that the size of the cavity is not too large, for instance by working far enough from the putative RFOT so that the point-to-set correlation length is not much bigger than the size of the atoms (which in practice is always the case in computer simulations), such a numerical experiment may then provide the information we are after: if the crossover between a high overlap with the reference configuration for a small cavity size to a small overlap for a large cavity size becomes sharper and takes place at an increasing length scale as one decreases the temperature, this is the sign that on the probed length scale, the finite-size system behaves according to the predicted RFOT scenario. It may still be hard to go from here to a determination of the parameters in the effective Ginzburg-Landau functional but it is enough to dismiss the alternative scenario with $w_2 < w_1$ and a (possibly avoided) continuous spin-glass transition.[11] In the latter case, the system constrained in a cavity would display a completely different behavior. In particular, in the first regime, when the point to set starts to grow, the overlap would always smoothly decrease as a function of the cavity size, without leading to a sharp crossover, and this behavior would be observed on a small, never increasing length scale for overlaps of the order of one. Only the tail at large cavity size would display a decrease to zero, characterized by a range growing as the spin-glass correlation length: this, however, is besides our goal of probing only the influence of the local fluctuations.[35] The published results of computer simulations of glass-forming liquids with the cavity method[34] point in favor of the RFOT scenario, giving credit to the effective RFOT functional as a bona fide starting point. Again, we reiterate that passing the test concerning the robustness with respect to the short-range fluctuations still does not guarantee the fate of the scenario at long distance when fluctuations on all scales are taken into account.

VII. CONCLUSION

In order to clarify the starting point for studying the effect of the fluctuations on the discontinuous glass transition (RFOT) found in infinite-dimensional (fully connected) glass models, we have analyzed disordered spin models characterized by interactions that couple spins on pairs of nearest-neighbor sites on a lattice. (This restriction to short-range two-site interactions was motivated by the fact that such models are amenable to real-space RG analyses and that they are easier

to study numerically than multisite interaction systems akin to the p-spin model.)

Proceeding along the way, we have disentangled two possible causes for destabilizing an RFOT in finite dimensions. The more obvious, which was anticipated, is that long-distance and, possibly, nonperturbative fluctuations could wipe out, or alter, the transition. The other one is that already accounting for short-range fluctuations, as the local effect of a finite number of neighbors, could drastically change the physics of a finite-dimensional system compared to its infinite-dimensional counterpart. Our present work is an assessment of the latter, which shows the fragility of the RFOT scenario to the effect of short-range fluctuations in the case of disordered spin models. This highlights how nontrivial is the step of deriving an effective theory for the RFOT phenomenology from a rigorous integration of the local short-range fluctuations.

We have identified and studied several mechanisms hampering the existence of a RFOT in finite (not too high) dimensional disordered spin models. For Potts glasses, the two-fold requirement of having (1) mainly antiferromagnetic couplings in order to avoid long-range ferromagnetic ordering and (2) a large number of states (or colors) in order to have a strongly discontinuous glass transition imposes that the lattice dimensionality has to be high, typically larger than the number of states. Otherwise, the model becomes unfrustrated and glassiness is wiped out. For instance, we have verified by using the Bethe approximation that the 10-states disordered Potts model studied by Brangian *et al.*[5] is not glassy in three dimensions. The other disordered models that we have considered, the M-p-spin models[14] with $M = p = 3$, and the F model introduced by us, which both display a RFOT in the infinite-dimensional limit, are characterized by a very small surface tension Y. As a consequence, we expect finite-dimensional fluctuations to be overwhelming compared to Y and to lead, in a RG sense, to a vanishing renormalized surface tension on larger length scales and, accordingly, to the absence of a glass transition. These results and the $1/d$ expansion performed for Potts glasses suggest that the perturbative regime in $1/d$ where (infinite-dimensional) mean-field results remain predictive is restricted to very high dimensions only.

We stress that we have nonetheless not found a fundamental principle or a general mechanism forbidding *a priori* the existence of a RFOT and of the associated glassy phenomenology in all possible disordered spin models involving only interactions between pairs of nearest-neighbor sites in realistic dimensions (e.g., $d = 3$). However, it is a fact—actually a puzzling one—that none of these models so far proposed display a RFOT beyond the large-dimensional limit. The RFOT theory originated from the analysis of disordered spin models. Somewhat ironically, structural glass physics turns out to lack robustness precisely in these models, whereas it appears instead to be less fragile at least to the effect of short-range fluctuations in liquid models.[36] Other simple statistical mechanical models for structural glasses have also been proposed that usually consider interactions that couple degrees of freedom on more than two sites, such as plaquette models[37] and variants (see also Refs. 38–41 for recent alternative proposals). Models with multisite interactions and no quenched disorder such as lattice-glass models do show the anticipated glassy behavior[42–44] even after that short range fluctuations are taken into account (by solving them within the Bethe approximation, for instance) and seem to provide a better starting point to study the effect of long-range fluctuations on the ideal glass transition. However, they are prone to simple long-range ordering, in particular, to crystallization. The addition of quenched disorder could then possibly prevent the formation of the crystalline phase without altering too much the glassy one.[45] In any case, we suggest that any new proposal should be first tested to assess the robustness of the RFOT to the effect of short-range fluctuations by, e.g., studying the Bethe approximation or similar procedures. The quest for a simple statistical mechanical model showing RFOT behavior is still open.

ACKNOWLEDGMENTS

We thank F. Caltagirone, U. Ferrari, F. Krzakala, L. Leuzzi, E. Marinari, M. Moore, G. Parisi, and T. Rizzo for discussions. GB, CC, and MT acknowledge financial support from the ERC grant NPRG-GLASS.

APPENDIX A: PROOF OF THE ABSENCE OF PHASE TRANSITION IN THE ANTIFERROMAGNETIC POTTS MODEL WITH RANDOM COLOR PERMUTATIONS ON EUCLIDEAN LATTICES

In this Appendix, we aim at proving, in the case of Euclidean lattices, the absence of phase transition in the antiferromagnetic q-state Potts model with random color permutations when the number of colors/states is large enough compared to the lattice coordination number. To do so, we generalize the proof given by Salas and Sokal[19] of the absence of phase transition for the antiferromagnetic Potts model and apply it to the disordered model with random color permutations (note that the Salas-Sokal proof also applies to a random-bond Potts model, provided all couplings are negative, i.e., antiferromagnetic). The Salas-Sokal demonstration makes use of the Dobrushin-Lanford-Ruelle approach to the equilibrium statistical mechanics of infinite volume classical lattice systems[46] and of Dobrushin's uniqueness theorem.[47] They show that the antiferromagnetic q-color Potts model on a lattice of maximum coordination number c has no phase transition (at any temperature $T \geqslant 0$) when $q > 2c$. Again, a large number of colors/states precludes the existence of a transition.

The antiferromagnetic Potts model with random permutations on a d-dimensional Euclidean lattice is defined by the following Hamiltonian:

$$H = J \sum_{\langle i,j \rangle} \delta_{\sigma_i, \pi_{ij}(\sigma_j)}, \tag{A1}$$

where $J > 0$, $\langle i,j \rangle$ denotes distinct pairs of nearest neighbors on the lattice, the spin variable σ can take q values $\{1,2,\ldots,q\}$, $\delta_{\sigma,\sigma'}$ is the Kronecker symbol, and π_{ij} is a random permutation of the q colors that is attached to the (oriented) edge between i and j. This model has a "gauge invariance" that prevents antiferromagnetic ordering;[8–10] indeed, if one permutes the states of the spin at a given site i, one can always find random permutations associated with all edges emanating from i such that the energy does not change; after averaging over

the quenched disorder (random permutations), the (staggered) magnetization is then zero.

Following the Salas-Sokal development, we introduce the conditional probability distribution for a single spin σ_i at site i with external conditions given by all other spins $\{\sigma_k\}'$ with $k \neq i$. The new ingredient is that this probability distribution is defined for a given realization $\boldsymbol{\pi}$ of the random permutations on all (oriented) edges of the infinite-volume lattice. It is given by the following Boltzmann-Gibbs measure:

$$P_{\boldsymbol{\pi}}(\sigma_i|\{\sigma_k\}') = Z_{\boldsymbol{\pi}}(\{\sigma_k\}')^{-1} \exp\left[-\beta J \sum_{k\neq i} \delta_{\sigma_i,\widehat{\pi}_{ik}(\sigma_k)}\right], \quad \text{(A2)}$$

where the *a priori* single-spin distributions over the colors are left implicit, $\beta = 1/(k_B T)$, and $\widehat{\pi}_{ik}$ is equal to π_{ik} if the edge is oriented from i to k and to π_{ki}^{-1} otherwise [we have used the fact that $\delta_{\sigma_k,\pi_{ki}(\sigma_i)} = \delta_{\sigma_i,\pi_{ki}^{-1}(\sigma_k)}$]. Note that, as the notations π is used for the random permutations, we have chosen P for the conditional probabilities, which is then different from the Salas-Sokal notation.[19]

We also introduce the quantity $c_{ij}^{\boldsymbol{\pi}}$ that measures the strength of the direct dependence between the spins on sites i and j:

$$c_{ij}^{\boldsymbol{\pi}} \equiv \sup_{\{\sigma\},\{\widetilde{\sigma}\}:\sigma_k=\widetilde{\sigma}_k \forall k\neq j} d[P_{\boldsymbol{\pi}}(\sigma_i|\{\sigma\}), P_{\boldsymbol{\pi}}(\sigma_i|\{\widetilde{\sigma}\})], \quad \text{(A3)}$$

where $d[,]$ is the distance between the conditional probability measures whose definition is irrelevant here.[19] It is easy to check that $c_{ij}^{\boldsymbol{\pi}} = 0$ when $i = j$ or when i and j are not nearest neighbors on the lattice. The interesting situation is therefore when j is one of the c nearest neighbors of i, which will be assumed from now on (we consider here a lattice of constant coordination number c but the reasoning works as well when c is the maximum coordination number).

Salas and Sokal[19] have proven a lemma which implies that

$$c_{ij}^{\boldsymbol{\pi}} \leqslant \max\left[\frac{\rho_i^{\boldsymbol{\pi}}[1-f_{ij}]}{\rho_i^{\boldsymbol{\pi}}[f_{ij}]}, \frac{\rho_i^{\boldsymbol{\pi}}[1-\tilde{f}_{ij}]}{\rho_i^{\boldsymbol{\pi}}[\tilde{f}_{ij}]}\right], \quad \text{(A4)}$$

where the functions f_{ij} and $\tilde{f}_{ij}$ are defined as

$$\begin{aligned} f_{ij}(\sigma_i|\sigma_j) &= \exp[-\beta J \delta_{\sigma_i,\widehat{\pi}_{ij}(\sigma_j)}], \\ \tilde{f}_{ij}(\sigma_i|\widetilde{\sigma}_j) &= \exp[-\beta J \delta_{\sigma_i,\widehat{\pi}_{ij}(\widetilde{\sigma}_j)}], \end{aligned} \quad \text{(A5)}$$

where $\widehat{\pi}_{ij}$ is defined from π_{ij} as above; $\rho_i^{\boldsymbol{\pi}}$ is the probability distribution at site i in the presence of all its nearest neighbors except j,

$$\rho_i^{\boldsymbol{\pi}}(\sigma_i) = \left(Z_i^{\boldsymbol{\pi}}\right)^{-1} \exp\left[-\beta J \sum_{k/i,k\neq j} \delta_{\sigma_i,\widehat{\pi}_{ik}(\sigma_k)}\right], \quad \text{(A6)}$$

where the notation k/i means that k is one of the c nearest neighbors of i and the normalization factor $Z_i^{\boldsymbol{\pi}}$ is the trace over the q distinct states/colors that the spin σ_i can take. Finally, $\rho_i^{\boldsymbol{\pi}}[f_{ij}]$ and $\rho_i^{\boldsymbol{\pi}}[f_{ij}]$ are short-hand notations for

$$\rho_i^{\boldsymbol{\pi}}[1-f_{ij}] = \sum_{\sigma_i=1}^{q} \rho_i^{\boldsymbol{\pi}}(\sigma_i)[1-f_{ij}(\sigma_i|\widetilde{\sigma}_j)], \quad \text{(A7)}$$

$$\rho_i^{\boldsymbol{\pi}}[f_{ij}] = \sum_{\sigma_i=1}^{q} \rho_i^{\boldsymbol{\pi}}(\sigma_i) f_{ij}(\sigma_i|\widetilde{\sigma}_j). \quad \text{(A8)}$$

Similar expressions hold for $\rho_i^{\boldsymbol{\pi}}[1-\tilde{f}_{ij}]$ and $\rho_i^{\boldsymbol{\pi}}[\tilde{f}_{ij}]$. The demonstration of the Salas-Sokal lemma requires that f_{ij} and $\tilde{f}_{ij}$ be in the interval $[0,1]$, which is verified when all couplings are antiferromagnetic as considered here.

Note that by construction, $\rho_i^{\boldsymbol{\pi}}[1-f_{ij}] + \rho_i^{\boldsymbol{\pi}}[f_{ij}] = 1$, so that

$$\frac{\rho_i^{\boldsymbol{\pi}}[1-f_{ij}]}{\rho_i^{\boldsymbol{\pi}}[f_{ij}]} = \frac{1}{\frac{1}{\rho_i^{\boldsymbol{\pi}}[1-f_{ij}]} - 1}, \quad \text{(A9)}$$

and, similarly, for the expression with $\tilde{f}_{ij}$.

The procedure now involves deriving an upper bound for $\rho_i^{\boldsymbol{\pi}}[1-f_{ij}]$ and $\rho_i^{\boldsymbol{\pi}}[1-\tilde{f}_{ij}]$. From Eqs. (A4) and (A9), this provides then an upper bound for $c_{ij}^{\boldsymbol{\pi}}$.

An upper bound for $\rho_i^{\boldsymbol{\pi}}[1-f_{ij}]$ is derived by noting first that from the definition of f_{ij} in Eq. (A5), the only nonzero contribution to the sum in Eq. (A7) comes from states such that $\sigma_i = \widehat{\pi}_{ij}(\sigma_j)$. There is only one such state. The next step is to find a bound for the contribution of any of the q states σ_i to the conditional probability distribution $\rho_i^{\boldsymbol{\pi}}$. Since $J > 0$, the maximum possible weight is when $\sum_{k/i,k\neq j} \delta_{\sigma_i,\widehat{\pi}_{ik}(\sigma_k)} = 0$. This occurs when σ_i is different from all $\widehat{\pi}_{ik}(\sigma_k)$'s with k any nearest neighbor of i different from j. Since there are $c-1$ such nearest neighbors, there are at most $q-(c-1)$ states with maximum weight. (The number of states is less when in the set $\{\widehat{\pi}_{ik}(\sigma_k)\}$ several colors are repeated.) The contribution of all the other states is strictly smaller. As a result the weight of any of the q states σ_i with the conditional probability distribution $\rho_i^{\boldsymbol{\pi}}$ is always less than $1/[q-(c-1)]$. Putting together the above results we arrive at the conclusion that $\rho_i^{\boldsymbol{\pi}}[1-f_{ij}] \leqslant 1/[q-(c-1)]$. From Eq. (A9), it then follows that

$$\frac{\rho_i^{\boldsymbol{\pi}}[1-f_{ij}]}{\rho_i^{\boldsymbol{\pi}}[f_{ij}]} \leqslant \frac{1}{q-c}, \quad \text{(A10)}$$

and, similarly, for the ratio involving $\tilde{f}_{ij}$.

One then concludes that for all pairs of nearest neighbors i, j on the lattice,

$$c_{ij}^{\boldsymbol{\pi}} \leqslant \frac{1}{q-c}. \quad \text{(A11)}$$

For any given realization of the quenched disorder, the so-called Dobrushin constant $\alpha^{\boldsymbol{\pi}} \equiv \sup_i \sum_{j\neq i} c_{ij}^{\boldsymbol{\pi}}$ therefore satisfies

$$\alpha^{\boldsymbol{\pi}} \leqslant \frac{c}{q-c}. \quad \text{(A12)}$$

The Dobrushin uniqueness theorem[47] states that there is a unique infinite-volume Gibbs measure when the condition $\alpha^{\boldsymbol{\pi}} < 1$ is satisfied. Under the same condition, an additional theorem implies that the correlations in the infinite-volume Gibbs measure decay exponentially with distance (see Ref. 19 and references therein). By using Eq. (A12), the above condition amounts to

$$q > 2c. \quad \text{(A13)}$$

This is true for any realization of the random permutations on the infinite-volume lattice. This proves the absence of phase transition and the exponential decay of the correlations, hence the absence of any glassy behavior, when the number of colors is larger than a threshold depending on the lattice coordination number.

APPENDIX B: THE POTTS MODEL ON RANDOM GRAPHS. ANALYTIC SOLUTION USING THE CAVITY METHOD

In this Appendix we report the main steps of the analytic solution of the Potts model on random graphs and explain briefly how the phase diagrams of Figs. 1 and 2 were derived. We refer to Refs. 10, 49, and 43 for more details. The Hamiltonian of the model as defined in Brangian *et al.*[5] is

$$\mathcal{H} = -\sum_{\langle i,j\rangle} J_{ij}\left(q\delta_{\sigma_i,\sigma_j} - 1\right), \tag{B1}$$

where $\langle i,j\rangle$ denotes the sum over all couples of nearest-neighbor sites of the lattice, and J_{ij} are quenched independent and identically distributed random variables extracted from the bimodal distributions, Eq. (4). The lattice we focus on is a random $(k+1)$-regular graph, i.e., a graph chosen uniformly at random among all graphs of N sites where each of the sites has connectivity $k+1$. The properties of such random graphs have been extensively studied in the past years. It is known in particular that any finite portion of the graph is a loopless tree with probability 1 in the thermodynamic limit, but there are large loops whose average size scales as $\ln N$. Random-regular graphs are like Cayley trees wrapped onto themselves. The advantage of this construction compared to infinite regular trees is the absence of boundary effects, which is particularly important for frustrated and disordered models.

The Potts model (B1) on a tree can be solved exactly by an iterative method called the cavity method, which is, in fact, a classical tool in statistical physics to deal with tree structures that dates back to the original ideas of Bethe, Peierls, and Onsager.[48] It allows one to compute the marginal probabilities that a given node is in a given state and observables such as energy, entropy, average magnetization, etc.

Denote $\psi_\alpha^{i\to j}$ the probability that the spin i is in state α when the edge (ij) is not present. Such a probability follows a recursion relation in terms of the marginal probabilities on the neighboring sites:

$$\psi_\alpha^{i\to j} = \frac{1}{Z_0^{i\to j}} \prod_{l\in\partial i/j} \left[(e^{\beta J_{il}(q-1)} - e^{-\beta J_{il}})\psi_\alpha^{l\to i} + e^{-\beta J_{il}}\right], \tag{B2}$$

where $Z_0^{i\to j}$ is a normalization constant insuring that $\sum_\alpha \psi_\alpha^{i\to j} = 1$ and is defined as

$$Z_0^{i\to j} = \sum_\alpha \prod_{l\in\partial i/j} \left[(e^{\beta J_{il}(q-1)} - e^{-\beta J_{il}})\psi_\alpha^{l\to i} + e^{-\beta J_{il}}\right]. \tag{B3}$$

To compute averages of observables over different quenched disorder realizations, we need to solve the self-consistent cavity functional equation

$$P(\{\psi_\alpha\}) = \int \mathrm{d}P(J_{il}) \int \prod_{l=1}^{k-1} \mathrm{d}P\left(\{\psi_\alpha^l\}\right)\delta\left[\psi_\alpha - \mathcal{F}\left(\{\psi_\alpha^l\}\right)\right], \tag{B4}$$

where $\mathcal{F}(\{\psi_\alpha^l\})$ denotes the right-hand side of Eq. (B2), and $P(J_{il})$ is the bimodal distribution of the coupling constants, Eq. (4). It is immediate to observe that $P(\{\psi_\alpha\}) = \delta(\psi_\alpha - 1/q)$ (i.e., each of the q components of each cavity field $\psi_\alpha^{i\to j}$ equals $1/q$), is always a solution of Eq. (B4). This solution corresponds to the RS paramagnetic phase and is the only solution at high temperature. The free energy density of the RS paramagnetic phase can be easily computed within the cavity method in the thermodynamic limit, as explained in Ref. 10. In the derivation of the equations above, we assumed that the cavity probabilities $\psi_\alpha^{l\to i}$ for the neighbors l of the node i are "sufficiently" independent in absence of the node i itself (only then does the joint probability factorize). This assumption would be true if the lattice were a tree with uncorrelated boundary conditions, but loops, or correlations in the boundaries, may create correlations between the neighbors of node i (even in absence of i) and the RS cavity assumption used above might thus cease to be valid in a general graph. A simple to compute, necessary but not sufficient, validity condition for the RS assumption is the nondivergence of the spin-glass susceptibility, $\chi_{\mathrm{SG}} = 1/N\sum_i \langle\sigma_i\sigma_j\rangle_c^2$. If the latter diverges, a spin-glass transition occurs, and the replica symmetry has to be broken. Using the fluctuation-dissipation theorem, we relate the correlation $\langle\sigma_i\sigma_j\rangle_c$ to the variation of magnetization in σ_i caused by an infinitesimal field in σ_j, which can be computed from the Jacobian evaluated at the RS paramagnetic solution (see Refs. 10 and 49):

$$T_{\alpha\beta} = \left.\frac{\partial\psi_\alpha^{i\to j}}{\partial\psi_\beta^{l\to i}}\right|_{\mathrm{RS}}. \tag{B5}$$

This matrix has only two different entries (all the diagonal elements are equal and all the nondiagonal elements are also equal) and only two distinct eigenvalues:

$$\begin{aligned}\lambda_1 &= \left.\left(\frac{\partial\psi_1^{i\to j}}{\partial\psi_1^{l\to i}} - \frac{\partial\psi_1^{i\to j}}{\partial\psi_2^{l\to i}}\right)\right|_{\mathrm{RS}},\\ \lambda_2 &= \left.\left(\frac{\partial\psi_1^{i\to j}}{\partial\psi_1^{l\to i}} + (q-1)\frac{\partial\psi_1^{i\to j}}{\partial\psi_2^{l\to i}}\right)\right|_{\mathrm{RS}}.\end{aligned} \tag{B6}$$

The second eigenvalue corresponds to a homogeneous eigenvector and describes fluctuations preserving the permutational symmetry among states. It is thus not likely to be the relevant one and, indeed, $\lambda_2 = 0$. The first eigenvalue is $(q-1)$-fold degenerate. Its eigenvectors correspond to fluctuations which explicitly break the permutational symmetry among states and are in fact the critical ones. By using the cavity recursion (B2), the two derivatives can be easily computed and the critical temperature below which the instability sets in can be obtained from the condition $k\overline{\lambda_1^2} = 1$ (see Refs. 10 and 49). This temperature corresponds to T_{local}, defined in the main text as the temperature at which the RS solution becomes unstable towards RSB (red line of Fig. 2).

Another important instability appears when $k|\lambda_1| = 1$. This corresponds to the instability towards the appearance of the usual ferromagnetic (if $\lambda_1 > 0$, red dashed line of Fig. 1) or antiferromagnetic (if $\lambda_1 < 0$, green line of Fig. 2) order, corresponding to the divergence of the magnetic susceptibilities related, respectively, to the breaking of the permutational symmetry among states or to the translational invariance *and* permutational symmetry. The condition $k|\lambda_1| = 1$ yields either the spinodal point of the PM phase with respect to the ordered one if the transition between the two is first order (T_{sp}, green line of Fig. 2) or the transition temperature between the PM and the ordered phase if the transition is second order. In the

case of Fig. 1, the transition between the paramagnetic phase and the ferromagnetic one is discontinuous. However, instead of plotting the spinodal line of the paramagnetic phase (which could be obtained from the stability condition as described above), we have plotted the transition line between the two phases (red dashed line of the figure), which corresponds to the set of points where the free energies of the two phases cross. Moreover, note that the antiferromagnetic (AF) solution is incompatible with the structure of the random graph defined above because of the existence of frustrating loops of arbitrary length. As a consequence, in order to analyze the AF phase, we have also considered bipartite random regular graphs (which are compatible with the AF order). We have solved Eq. (B2) on such a bipartite graph, computed the free energy associated to the AF phase, and compared it with the other solutions.

So far, we have described the RS cavity method. This method does not allow one to describe the glass and the spin-glass phases, since it neglects the possibility of the existence of several pure states in which the Gibbs measure is decomposed. In order to take into account the existence of several pure states, a one-step replica symmetry breaking (1RSB) cavity formalism is necessary. In general, dealing with exponentially many pure states is a nightmare for all known rigorous approaches in the thermodynamic limit. The heuristic cavity method overcomes this problem elegantly, as was shown originally in the seminal work of Ref. 49. A detailed description of the 1RSB cavity solution goes beyond the scope of this work, and we refer to Refs. 10, 43, and 49 for more details. The different pure states correspond to the different fixed points of Eq. (B2). The goal is thus to analyze the statistical properties of these fixed points. Each one of the states is weighted by the corresponding free energy to the power m, where m is just a parameter analogous to the inverse temperature. The probability measure over states $\{\psi\}$ is then

$$\mu(\{\psi\}) = \frac{1}{Z_1} e^{-\beta m N f(\{\psi\})}, \tag{B7}$$

where Z_1 is a normalization constant. One can show that, once the average over different pure states is performed, the analog of the recursion equations (B2) becomes

$$P^{i\to j}\big(\{\psi_\alpha^{i\to j}\}\big) = \frac{1}{Z_1^{i\to j}} \int \prod_{l\in\partial i/j} \mathrm{d}P^{l\to i}\big(\{\psi_\alpha^{l\to i}\}\big) \times \delta\big[\psi_\alpha^{i\to j} - \mathcal{F}\big(\{\psi_\alpha^{l\to i}\}\big)\big]\big(Z_0^{i\to j}\big)^m, \tag{B8}$$

where $Z_0^{i\to j}$ has been defined by Eq. (B3). In order to compute averages of observables over different quenched disorder realizations, we need to introduce the probability distribution $\mathcal{Q}[P^{i\to j}(\{\psi_\alpha^{i\to j}\})]$ and solve the following self-consistent 1RSB cavity functional equation:

$$\mathcal{Q}\big[P^{i\to j}\big(\{\psi_\alpha^{i\to j}\}\big)\big] = \int \mathrm{d}P(J_{il}) \int \prod_{l=1}^{k-1} \mathrm{d}\mathcal{Q}\big[P\big(\{\psi_\alpha^{l\to i}\}\big)\big] \delta\big[P^{i\to j}\big(\{\psi_\alpha^{i\to j}\}\big) - \mathcal{F}_1\big(\{P^{l\to i}\big(\{\psi_\alpha^{l\to i}\}\big)\}\big)\big], \tag{B9}$$

where $\mathcal{F}_1(\{P^{l\to i}(\{\psi_\alpha^{l\to i}\})\})$ is the right-hand side of Eq. (B8). Once the fixed point of the above equation is found, the replicated 1RSB free energy of the glass phase can be computed.[10,49] In principle, Eq. (B9) could be solved using the population dynamics algorithm[10,49] with arbitrary numerical precision, by representing the probability distribution $\mathcal{Q}[P^{i\to j}(\{\psi_\alpha^{i\to j}\})]$ with a population of populations of q-components fields $\{\psi_\alpha^{i\to j}\}$. Numerical precision is thus limited by populations' sizes (our numerical solutions of Eq. (B9) has been obtained with a population of 2^{12} populations of 2^{12} fields). Three different cases are then observed: (a) At high enough temperature, there is only the trivial (RS) solution at $m = 1$ of Eq. (B9). Then the RS approach is correct and the system is in the paramagnetic phase. (b) As the temperature is lowered, a nontrivial solution at $m = 1$ appears, and $m = 1$ yields the minimum of the total free energy (this corresponds to a positive configurational entropy associated with the pure states). This is not a true thermodynamic transition, since the correct solution is still given by the RS one. However, the phase space is broken into exponentially many components and, as a consequence, the dynamics fall out-of-equilibrium. Thus, the highest temperature where a nontrivial solution of Eq. (B9) at $m = 1$ first appears corresponds to the dynamical critical temperature T_d (blue dashed line of Fig. 2). (c) As the temperature is further decreased, the minimum of the total free energy is found for $0 < m^\star < 1$ (this corresponds to a negative configurational entropy). The system is in the ideal glass phase. The Kauzmann temperature T_K, where a genuine thermodynamic transition takes place, is defined as the temperature at which $m^\star \to 1$. Note that when a continuous transition from the paramagnetic phase to the spin-glass one occurs, one observes a direct transition from case (a) to case (c). Then the dynamical transition temperature T_d and the Kauzmann one T_K coincide, and they are also equal to T_{local}.

We conclude this Appendix with a discussion about the numerical uncertainty on the location of the transition lines shown in Figs. 1 and 2. There are three sources of error which are, respectively, due to (1) finite number of iteration of the cavity equations, (2) finite population size, and (3) dichotomy procedure. The first source is due to the fact that in order to find the fixed point solution of the cavity equations one solves them by iteration; in the limit of an infinite number of iterations the fixed point is reached but, in practice, one is bound to only do a finite number of them (we performed between 10^2 and 10^3 iterations). This introduces an error which is quite small since the convergence is exponential except for the spin-glass phase where it is power-law-like. The second source of error is the finite size of the population used to reproduce the probability distribution. This leads to an error that scales as the inverse of the square root of the population size. Finally, for the dynamical transition only, a third source of error is present: the transition corresponds to the limiting point at which the $m = 1$ RSB solution disappears. This is found by dichotomy by reducing progressively the interval to which the transition point belongs. In consequence, there is unavoidably an uncertainty in the location of the transition due to the size of the interval corresponding to the stopping of the numerical dichotomy procedure. The error bars drawn in Figs. 1 and 2 are obtained by taking into account all these sources of error.

APPENDIX C: THE 1/d EXPANSION FOR THE POTTS MODEL

As discussed in the main text, we use the simplex representation of the Potts glass:

$$H = -\sum_{\langle i,j\rangle} J_{ij} \sum_{a=1}^{q-1} S_{i,a} S_{j,a}. \tag{C1}$$

In this representation, q is the number of colors and the degrees of freedom $S_{i,a}$ are vectors pointing toward the q vertices of a thetrahedron in a $(q-1)$-dimensional space. These vectors satisfy the following relations:

$$\sum_{s=1}^{q} e_a^s e_b^s = q\,\delta_{ab}, \tag{C2}$$

$$\sum_{a=1}^{q-1} e_a^s e_a^{s'} = q\,\delta_{ss'} - 1, \tag{C3}$$

$$\sum_{s=1}^{q} e_a^s = 0, \tag{C4}$$

$$\left(\sum_{a=1}^{q-1} e_a^s e_a^{s'}\right)^2 = (q-2)\sum_{a=1}^{q-1} e_a^s e_a^{s'} + q - 1. \tag{C5}$$

Integration of the partition function replicated n times over the quenched disorder gives

$$\overline{Z^n} = \sum_{\{s^\alpha\}} \prod_{\langle i,j\rangle} \exp\left[\frac{\beta^2}{2d}\sum_{(\alpha,\beta)}\sum_{a,b} S_{i,a}^\alpha S_{i,b}^\beta S_{j,a}^\alpha S_{j,b}^\beta + \beta\tilde{J}_0 \sum_\alpha \sum_a S_{i,a}^\alpha S_{j,a}^\alpha\right], \tag{C6}$$

1. Large-dimension (or large-temperature) expansion

The large-dimension expansion is a kind of high-temperature expansion, as discussed by Georges and Yedidia.[22] Following Refs. 21 and 22, we introduce a small parameter υ in front of the terms that couples different sites. We also introduce two sets of Lagrange multipliers $\lambda_i^{\alpha\beta}$ and η_i^α to ensure that the following relations hold for each value of the small parameter υ:

$$\left\langle S_{i,a}^\alpha S_{i,b}^\beta \right\rangle = \delta_{ab}\, Q_i^{\alpha\beta} \tag{C7}$$

and

$$\left\langle S_{i,a}^\alpha \right\rangle = m_i^\alpha. \tag{C8}$$

As a result, we have

$$-\beta A\left(\left\{Q_i^{\alpha\beta}\right\},\left\{m_i^\alpha\right\};\left\{\lambda_i^{\alpha\beta}\right\},\left\{\eta_i^\alpha\right\}\right) = \ln \mathrm{Tr}_{\{S^\alpha\}} \exp\left\{\upsilon H + \sum_i \sum_{\alpha,\beta} \lambda_i^{\alpha\beta}\left[\sum_a S_{i,a}^\alpha S_{i,a}^\beta - (q-1)q_i^{\alpha\beta}\right] + \sum_i \sum_\alpha \eta_i^\alpha\left[\sum_a S_{i,a}^\alpha - (q-1)m_i^\alpha\right]\right\}, \tag{C9}$$

where N is the number of sites in the system and

$$H = \frac{\beta^2}{2d}\sum_{(i,j)}\sum_{(\alpha,\beta)}\sum_{a,b} S_{i,a}^\alpha S_{i,b}^\beta S_{j,a}^\alpha S_{j,a}^\beta + \beta\tilde{J}_0 \sum_{(i,j)}\sum_\alpha\sum_a S_{i,a}^\alpha S_{j,a}^\alpha.$$

We have implicitly assumed that by symmetry

$$Q_{i,ab}^{\alpha\beta} = \delta_{ab} Q_i^{\alpha\beta} \forall a$$

and

$$m_{i,a}^{\alpha\beta} = m_i^\alpha \forall a.$$

To preserve the relations in Eqs. (C7) and (C8) we impose, $\lambda_i^{\alpha\beta}$ so that

$$\frac{\partial A}{\partial \lambda_i^{\alpha\beta}} = 0, \quad \text{which gives} \quad Q_i^{\alpha\beta} = \frac{1}{q-1}\sum_a S_{i,a}^\alpha S_{i,a}^\beta, \tag{C10}$$

and η_i^α so that

$$\frac{\partial A}{\partial \eta_i^\alpha} = 0, \quad \text{which gives} \quad m_i^\alpha = \frac{1}{q-1}\sum_a S_{i,a}^\alpha. \tag{C11}$$

A large-temperature/large-dimension expansion of $-\beta A$ can be obtained expanding $\exp(\upsilon H)$ around $\upsilon = 0$ and putting $\upsilon = 1$ at the end.[21] The terms of the expansion are expressed in terms of averages $\langle\ \rangle_0$ with the same weight as in Eq. (C9), except that

υ is set to zero:

$$\langle \mathcal{O}(\{S^\alpha\})\rangle_0 = \mathrm{Tr}_{\{S^\alpha\}}\left(\exp\left\{\sum_i\sum_{\alpha,\beta}\lambda_i^{\alpha\beta}\left[\sum_a S_{i,a}^\alpha S_{i,a}^\beta - (q-1)Q_i^{\alpha\beta}\right] + \sum_i\sum_\alpha \eta_i^\alpha\left[\sum_a S_{i,a}^\alpha - (q-1)m_i^\alpha\right]\right\}\mathcal{O}\right)\Big/ Z_0, \tag{C12}$$

where

$$Z_0 = \mathrm{Tr}_{\{S^\alpha\}}\exp\left\{\sum_i\sum_{\alpha,\beta}\lambda_i^{\alpha\beta}\left[\sum_a S_{i,a}^\alpha S_{i,a}^\beta - (q-1)Q_i^{\alpha\beta}\right] + \sum_i\sum_\alpha \eta_i^\alpha\left[\sum_a S_{i,a}^\alpha - (q-1)m_i^\alpha\right]\right\}. \tag{C13}$$

The expansion is of the form

$$A = A_0 + A_1\upsilon + \tfrac{1}{2}A_2\upsilon^2 + \cdots \tag{C14}$$

with, at the zeroth order,

$$-\beta A_0 = (-\beta A)|_0 = \ln Z_0, \tag{C15}$$

and at the first order,

$$-\beta A_1 = \left.\frac{\partial(-\beta A)}{\partial\upsilon}\right|_0. \tag{C16}$$

Then,

$$-\beta A_1 = \langle H\rangle = \frac{\beta^2}{2d}\sum_{(i,j)}\sum_{(\alpha,\beta)}\sum_{a,b}\left\langle S_{i,a}^\alpha S_{i,b}^\beta S_{j,a}^\alpha S_{j,b}^\beta\right\rangle_0 + \beta\tilde{J}_0\sum_{(i,j)}\sum_\alpha\sum_a\left\langle S_{i,a}^\alpha S_{j,a}^\alpha\right\rangle_0 \tag{C17}$$

and by using Eq. (C7), we obtain that $-\beta A_1$ is equal to

$$\frac{\beta^2}{2d}(q-1)\sum_{\langle i,j\rangle}\sum_{(\alpha,\beta)}Q_i^{\alpha\beta}Q_j^{\alpha\beta} + \beta\tilde{J}_0(q-1)\sum_{\langle i,j\rangle}\sum_\alpha m_i^\alpha m_j^\alpha.$$

To more easily compute the second order, we introduce the operator

$$\mathcal{U} = H - \langle H\rangle + \sum_i\sum_{(\alpha,\beta)}\frac{\partial\lambda_i^{\alpha\beta}}{\partial\upsilon}\left[\sum_a S_{i,a}^\alpha S_{i,a}^\beta - (q-1)Q_i^{\alpha\beta}\right] + \sum_i\sum_\alpha\frac{\partial\eta_i^\alpha}{\partial\upsilon}\left[\sum_a S_{i,a}^\alpha - (q-1)m_i^\alpha\right], \tag{C18}$$

which is such that

$$\frac{\partial\langle\mathcal{O}\rangle}{\partial\upsilon} = \left\langle\frac{\partial\mathcal{O}}{\partial\upsilon}\right\rangle + \langle\mathcal{O}\mathcal{U}\rangle. \tag{C19}$$

Useful properties of the operator $\mathcal{U}$ are listed in Ref. 21. The term A_2 can be written as

$$-\beta A_2 = \left.\frac{\partial^2(-\beta A)}{\partial\upsilon^2}\right|_0 = \langle\mathcal{U}_0^2\rangle_0\ , \tag{C20}$$

where $\mathcal{U}_0$ is the operator $\mathcal{U}$ such that all the averages it contains are those with $\upsilon = 0$ in the weight. Focusing on the $m = 0$ case (no ferromagnetic ordering), we get

$$-\frac{1}{2}\beta A_2 = \sum_{\langle i,j\rangle}\left[\frac{\beta^4}{8d^2}\sum_{\substack{(\alpha,\beta)\\(\gamma,\delta)}}\sum_{\substack{a,b\\c,d}}\left(\left\langle S_{i,a}^\alpha S_{i,b}^\beta S_{i,c}^\gamma S_{i,d}^\delta\right\rangle_0 - \delta_{ab}\delta_{cd}Q_i^{\alpha\beta}Q_i^{\gamma\delta}\right)\left(\left\langle S_{j,a}^\alpha S_{j,b}^\beta S_{j,c}^\gamma S_{j,d}^\delta\right\rangle_0 - \delta_{ab}\delta_{cd}Q_j^{\alpha\beta}Q_j^{\gamma\delta}\right)\right.$$

$$\left. + \frac{\beta^2}{2d}\beta\tilde{J}_0\sum_{\substack{(\alpha,\beta)\\\gamma}}\sum_{\substack{a,b\\c}}\left\langle S_{i,a}^\alpha S_{i,b}^\beta S_{i,c}^\gamma\right\rangle_0\left\langle S_{j,a}^\alpha S_{j,b}^\beta S_{j,c}^\gamma\right\rangle_0 + \frac{1}{2}(\beta\tilde{J}_0)^2\sum_{\alpha\neq\beta}(q-1)Q_i^{\alpha\beta}Q_j^{\alpha\beta}\right], \tag{C21}$$

as in the last sum the terms with $\alpha = \beta$ give only a constant.

2. Zeroth- and first-order terms

The first-order term is directly obtained as

$$-\beta A_1 = \frac{\beta^2}{2d} \sum_{\langle i,j \rangle} \sum_{(\alpha,\beta)} (q-1) Q_i^{\alpha\beta} Q_j^{\alpha\beta}. \tag{C22}$$

On the other hand, the zeroth-order term reads

$$-\beta A_0 = \ln \mathrm{Tr}_{\{S^\alpha\}} \exp \left\{ \sum_i \sum_{(\alpha,\beta)} \lambda_i^{\alpha\beta} \left[\sum_a S_{i,a}^\alpha S_{i,a}^\beta - (q-1) Q_i^{\alpha\beta} \right] \right\}. \tag{C23}$$

In the following, we compute this expression in an expansion in $\lambda_i^{\alpha\beta}$ and $Q_i^{\alpha\beta}$. First, we pull out the term not involved in the trace, which gives

$$-\beta A_0 = -\sum_i \sum_{(\alpha,\beta)} (q-1) \lambda_i^{\alpha\beta} Q_i^{\alpha\beta} + \ln \mathrm{Tr}_{\{S^\alpha\}} \prod_i \exp \left(\sum_{(\alpha,\beta)} \lambda_i^{\alpha\beta} \sum_a S_{i,a}^\alpha S_{i,a}^\beta \right). \tag{C24}$$

Next, we expand the argument of the trace to cubic order in the λ_i's:

$$\ln \mathrm{Tr}_{\{S^\alpha\}} \prod_i \exp \left(\sum_{(\alpha,\beta)} \lambda_i^{\alpha\beta} \sum_a S_{i,a}^\alpha S_{i,a}^\beta \right) = \ln \prod_i \mathrm{Tr}_{\{S_i^\alpha\}} \left(1 + \sum_{(\alpha,\beta)} \lambda_i^{\alpha\beta} \sum_a S_{i,a}^\alpha S_{i,a}^\beta + \frac{1}{2} \sum_{\substack{(\alpha,\beta) \\ (\gamma,\delta)}} \lambda_i^{\alpha\beta} \lambda_i^{\gamma\delta} \sum_{a,c} S_{i,a}^\alpha S_{i,a}^\beta S_{i,c}^\gamma S_{i,c}^\delta \right.$$
$$\left. + \frac{1}{6} \sum_{\substack{(\alpha,\beta) \\ (\gamma,\delta) \\ (\epsilon,\zeta)}} \lambda_i^{\alpha\beta} \lambda_i^{\gamma\delta} \lambda_i^{\epsilon\zeta} \sum_{a,c,e} S_{i,a}^\alpha S_{i,a}^\beta S_{i,c}^\gamma S_{i,c}^\delta S_{i,e}^\epsilon S_{i,e}^\zeta \right). \tag{C25}$$

From Eqs. (C2) and (C4), it is easily realized that one has to pair the replicas to obtain nonzero contributions from the trace. As a result, we find

$$\mathrm{Tr}_{\{S^\alpha\}} \sum_{(\alpha,\beta)} \lambda^{\alpha\beta} \sum_a S_a^\alpha S_a^\beta = 0, \tag{C26}$$

$$\frac{1}{2} \mathrm{Tr}_{\{S^\alpha\}} \sum_{\substack{(\alpha,\beta) \\ (\gamma,\delta)}} \lambda^{\alpha\beta} \lambda^{\gamma\delta} \sum_{a,c} S_a^\alpha S_a^\beta S_c^\gamma S_c^\delta = \frac{1}{2} \sum_{(\alpha,\beta)} (\lambda^{\alpha\beta})^2 (q-1) q^n \tag{C27}$$

and

$$\frac{1}{6} \mathrm{Tr}_{\{S^\alpha\}} \sum_{\substack{(\alpha,\beta) \\ (\gamma,\delta) \\ (\epsilon,\zeta)}} \lambda^{\alpha\beta} \lambda^{\gamma\delta} \lambda^{\epsilon\zeta} \sum_{a,c,e} S_a^\alpha S_a^\beta S_c^\gamma S_c^\delta S_e^\epsilon S_e^\zeta = \frac{1}{6} \sum_{(\alpha,\beta)} (\lambda^{\alpha\beta})^3 (q-1)(q-2) q^n + \frac{1}{6} \mathrm{Tr} \lambda^3 (q-1) q^n,$$

where we have used Eq. (C2) and

$$\sum_{a,b,c} \left(\sum_{s=1}^q e_a^s e_b^s e_c^s \right)^2 = (q-1)(q-2)/q^2. \tag{C28}$$

Finally, the expression of the zeroth-order contribution is obtained to a $O(\lambda^4)$ as

$$-\beta A_0 = N(q-1) \left[-\sum_{(\alpha,\beta)} \lambda^{\alpha\beta} Q^{\alpha\beta} + n \ln q + \frac{1}{2} \sum_{(\alpha,\beta)} (\lambda^{\alpha\beta})^2 + \frac{q-2}{6} \sum_{(\alpha,\beta)} (\lambda^{\alpha\beta})^3 + \frac{1}{6} \mathrm{Tr} \lambda^3 \right]. \tag{C29}$$

3. Second order

We start with Eq. (C21). To compute this expression as a function of $\lambda_i^{\alpha\beta}$ and $Q_i^{\alpha\beta}$, we again expand the weight in $\langle\,\rangle_0$ around $\lambda^{\alpha\beta}=0$ to a $O(\lambda^4)$. The only contributions that can be nonzero involve

$$\mathcal{S}_3^{\alpha\beta\gamma}=\left\langle S_{i,a}^{\alpha}S_{i,b}^{\beta}S_{i,c}^{\gamma}\right\rangle_0 \tag{C30}$$

with $\alpha\neq\beta$, for
(1) $\gamma\neq\alpha$ and $\gamma\neq\beta$,
(2) $\gamma=\alpha$ and $\gamma\neq\beta$,
and

$$\mathcal{S}_4^{\alpha\beta\gamma\delta}=\left\langle S_{i,a}^{\alpha}S_{i,b}^{\beta}S_{i,c}^{\gamma}S_{i,d}^{\delta}\right\rangle_0 \tag{C31}$$

with $\alpha\neq\beta$ and $\gamma\neq\delta$, for
(1) $\gamma\neq\alpha$, $\delta\neq\alpha$, $\gamma\neq\beta$, and $\delta\neq\beta$,
(2) $\gamma=\alpha$ and $\delta\neq\beta$,
(3) $\gamma=\alpha$ and $\delta=\beta$.

In the end, we need an expression that is cubic in the $Q_i^{\alpha\beta}$'s. For each term, we therefore make an expansion up to the third order in $\lambda_i^{\alpha\beta}$ at most. The detailed computation is quite cumbersome. Here, we only present the results term by term.

Let us start with the first term, $\mathcal{S}_3^{\alpha\beta\gamma}=\langle S_a^{\alpha}S_b^{\beta}S_c^{\gamma}\rangle_0$ with $\alpha\neq\beta$. (1) When $\gamma\neq\alpha$ and $\gamma\neq\beta$, the terms of order $O(1)$ and $O(\lambda)$ are zero. Hence one only has terms of order $O(\lambda^2)$ that become of order $O(\lambda^4)$ when the square is taken in the Gibbs free energy and can therefore be neglected. (2) When $\gamma=\alpha$, the only term of order $O(1)$ is zero, and we thus have to compute terms of order $O(\lambda)$ and $O(\lambda^2)$. We find that the linear term $\mathcal{S}_{3,\lambda}^{\alpha\beta\alpha}$ reads

$$q^{-1}\lambda^{\alpha\beta}\sum_S S_a^{\alpha}S_b^{\alpha}S_c^{\alpha}, \tag{C32}$$

whereas the quadratic term $\mathcal{S}_{3,\lambda^2}^{\alpha\beta}$ reads

$$\frac{1}{2}p^{-2}(\lambda^{\alpha\beta})^2\sum_{a_1,a_2}\left(\sum_S S_a^{\alpha}S_c^{\alpha}S_{a_1}^{\alpha}S_{a_2}^{\alpha}\right)\left(\sum_S S_b^{\beta}S_{a_1}^{\beta}S_{a_2}^{\beta}\right)+q^{-1}\sum_{\substack{\eta\neq\alpha\\ \eta\neq\beta}}\lambda^{\alpha\eta}\lambda^{\eta\beta}\left(\sum_S S_a^{\alpha}S_b^{\alpha}S_c^{\alpha}\right).$$

Now we consider the terms from $\mathcal{S}_4^{\alpha\beta\gamma\delta}=\langle S_a^{\alpha}S_b^{\beta}S_c^{\gamma}S_d^{\delta}\rangle_0$ with $\alpha\neq\beta$ and $\gamma\neq\delta$. (1) When $\gamma\neq\alpha$, $\gamma\neq\beta$, $\delta\neq\alpha$, and $\delta\neq\beta$, the terms of order $O(1)$ and $O(\lambda)$ are zero and there is no need to compute the term of order $O(\lambda^2)$. (2) When $\gamma=\alpha$ and $\delta\neq\beta$, the term of order $O(1)$ is zero but not the term of order $O(\lambda)$:

$$\mathcal{S}_{4,\lambda}^{\alpha\beta\alpha\delta}=\lambda^{\beta\delta}\delta_{ac}\delta_{bd}. \tag{C33}$$

(3) For the quadratic term, there are several contributions that will be denoted according to the way spins are grouped in the sums:

$$\mathcal{S}_{4,\lambda^2}^{\alpha\beta\alpha\delta}(4,2,2)=q^{-1}\lambda^{\alpha\beta}\lambda^{\alpha\delta}\left(\sum_S S_a^{\alpha}S_b^{\alpha}S_c^{\alpha}S_d^{\alpha}\right), \tag{C34}$$

$$\mathcal{S}_{4,\lambda^2}^{\alpha\beta\alpha\delta}(3,3,2)=q^{-2}\lambda^{\beta\delta}(\lambda^{\alpha\beta}+\lambda^{\alpha\delta})\sum_{a_1}\left(\sum_S S_a^{\alpha}S_c^{\alpha}S_{a_1}^{\alpha}\right)\times\left(\sum_S S_b^{\beta}S_d^{\beta}S_{a_1}^{\beta}\right), \tag{C35}$$

$$\mathcal{S}_{4,\lambda^2}^{\alpha\beta\alpha\delta}(2,3,3)=\frac{1}{2}q^{-2}(\lambda^{\beta\delta})^2\delta_{ac}\sum_{a_1,a_2}\left(\sum_S S_b^{\beta}S_{a_1}^{\beta}S_{a_2}^{\beta}\right)\times\left(\sum_S S_d^{\delta}S_{a_1}^{\delta}S_{a_2}^{\delta}\right), \tag{C36}$$

$$\mathcal{S}_{4,\lambda^2}^{\alpha\beta\alpha\delta}(2,2,2,2)=\sum_{\substack{\eta\neq\alpha\\ \eta\neq\beta\\ \eta\neq\delta}}\lambda^{\beta\eta}\lambda^{\eta\delta}\delta_{ac}\delta_{bd}. \tag{C37}$$

(4) When $\gamma=\alpha$ and $\delta=\beta$, all terms are nonzero. The term of order $O(1)$ is given by

$$\mathcal{S}_{4,1}^{\alpha\beta\alpha\beta}=\mathrm{Tr}_{S^{\alpha}}S_a^{\alpha}S_c^{\alpha}S_b^{\beta}S_d^{\beta}=\delta_{ac}\delta_{bd}. \tag{C38}$$

Note that it is not needed to go to the term of order $O(\lambda^3)$ because

$$\langle\,\rangle_0^2=(\langle\,\rangle_0-\delta_{ac}\delta_{bd}+\delta_{ac}\delta_{bd})^2=(\langle\,\rangle_0-\delta_{ac}\delta_{bd})^2+2\delta_{ac}\delta_{bd}(\langle\,\rangle_0-\delta_{ac}\delta_{bd})+(\delta_{ac}\delta_{bd})^2. \tag{C39}$$

Since $\delta_{ac}\delta_{bd}\langle\,\rangle_0$ is a constant, only the first term matters and computing the term $\langle\,\rangle_0$ to the order $O(\lambda^2)$ is enough to give a result of order $O(\lambda^3)$.

The linear term reads

$$\mathcal{S}_{4,\lambda}^{\alpha\beta\alpha\beta}=q^{-2}\lambda^{\alpha\beta}\sum_{a_1}\left(\sum_S S_a^{\alpha}S_c^{\alpha}S_{a_1}^{\alpha}\right)\left(\sum_S S_b^{\beta}S_d^{\beta}S_{a_1}^{\beta}\right). \tag{C40}$$

For the quadratic one, we find several contributions:

$$\mathcal{S}_{4,\lambda^2}^{\alpha\beta\alpha\beta}(4,4)=\frac{1}{2}q^{-2}(\lambda^{\alpha\beta})^{\times}\sum_{a_1,a_2}\left(\sum_S S_a^{\alpha}S_c^{\alpha}S_{a_1}^{\alpha}S_{a_2}^{\alpha}\right)\times\left(\sum_S S_b^{\beta}S_d^{\beta}S_{a_1}^{\beta}S_{a_2}^{\beta}\right), \tag{C41}$$

$$\mathcal{S}_{4,\lambda^2}^{\alpha\beta\alpha\beta}(4,2,2)=\frac{1}{2}(q-1)\delta_{ac}\delta_{bd}\left[\sum_{\eta\neq\alpha}(\lambda^{\beta\eta})^2+\sum_{\eta\neq\beta}(\lambda^{\alpha\eta})^2\right], \tag{C42}$$

$$\mathcal{S}_{4,\lambda^2}^{\alpha\beta\alpha\beta}(3,3,2)=q^{-2}\sum_{\substack{\eta\neq\alpha\\ \eta\neq\beta}}\lambda^{\alpha\eta}\lambda^{\eta\beta}\sum_{a_1}\left(\sum_S S_a^{\alpha}S_c^{\alpha}S_{a_1}^{\alpha}\right)\times\left(\sum_S S_b^{\beta}S_d^{\beta}S_{a_1}^{\beta}\right). \tag{C43}$$

4. The Gibbs free energy

In Eq. (C21), one has to consider the following terms:

$$\mathbf{S}_3 = \sum_{\substack{(\alpha,\beta)\\ \gamma}} \sum_{\substack{a,b\\ c}} \langle S_a^\alpha S_b^\beta S_c^\gamma \rangle_0^2, \tag{C44}$$

$$\mathbf{S}_4 = \sum_{\substack{(\alpha,\beta)\\ (\gamma,\delta)}} \sum_{\substack{a,b\\ c,d}} \langle S_a^\alpha S_b^\beta S_c^\gamma S_d^\delta \rangle_0^2, \tag{C45}$$

$$\mathbf{T}_4 = \sum_{\substack{(\alpha,\beta)\\ (\gamma,\delta)}} \sum_{\substack{a,b\\ c,d}} \delta_{ac}\delta_{bd} Q^{\alpha\beta} Q^{\gamma\delta} \langle S_a^\alpha S_b^\beta S_c^\gamma S_d^\delta \rangle_0. \tag{C46}$$

To compute these terms, we use the relations obtained in Ref. 23 where after introducing

$$v_{abc} = \left(\sum_S S_a S_b S_c \right) \tag{C47}$$

and

$$F_{abcd} = \left(\sum_S S_a S_b S_c S_d \right) \tag{C48}$$

and using the Einstein convention of summing over repeated indices, one has

$$v_{abc} v_{ade} = q F_{bcde} - q^2 \delta_{bc}\delta_{de}, \tag{C49}$$

$$v_{abc} v_{abd} = q^2(q-1)\delta_{cd}, \tag{C50}$$

$$v_{abc}^2 = q^2(q-1)(q-2), \tag{C51}$$

$$F_{aabc} = q(q-1)\delta_{bc}, \tag{C52}$$

$$F_{aabb} = q(q-1)^2, \tag{C53}$$

$$F_{abcd} F_{abef} = q^2 \left(\frac{q-2}{q} F_{cdef} + \delta_{cd}\delta_{ef} \right), \tag{C54}$$

$$F_{abcd}^2 = q^2(q-1)(q^2-3q+3), \tag{C55}$$

from which it also follows that

$$\delta_{ab}\delta_{cd} v_{abe} v_{cde} = 0. \tag{C56}$$

In Eq. (C44), only the terms in which $\alpha = \gamma$ or $\beta = \gamma$ are different from zero. This means that

$$\mathbf{S}_3 = \sum_{\alpha\neq\beta} \sum_{\substack{a,b\\ c}} \langle S_a^\alpha S_b^\beta S_c^\alpha \rangle_0^2. \tag{C57}$$

After substituting the terms of order $O(\lambda)$ and $O(\lambda^2)$, one finds

$$\mathbf{S}_3 = \sum_{\alpha\neq\beta} \sum_{\substack{a,b\\ c}} \left[q^{-1}\lambda^{\alpha\beta} v_{abc} + \frac{1}{2} q^{-2} (\lambda^{\alpha\beta})^2 \sum_{a_1,a_2} F_{aca_1a_2} v_{ba_1a_2} + q^{-1} \sum_{\substack{\eta\neq\alpha\\ \eta\neq\beta}} \lambda^{\alpha\eta}\lambda^{\eta\beta} v_{abc} \right]^2, \tag{C58}$$

which finally gives

$$\mathbf{S}_3 = (q-1)(q-2)\sum_{\alpha\neq\beta} (\lambda^{\alpha\beta})^2 + (q-1)(q-2)^2 \sum_{\alpha\neq\beta} (\lambda^{\alpha\beta})^3 + 2(q-1)(q-2)\mathrm{Tr}(\lambda^3). \tag{C59}$$

In Eq. (C45), the nonzero terms are those for which γ or δ is equal to α or β, while the other is different from both, or such that γ and δ are equal to α and β. Hence we have

$$\mathbf{S}_4 = \mathbf{S}_4^a + \mathbf{S}_4^b, \tag{C60}$$

where

$$\mathbf{S}_4^a = \sum_{\substack{\alpha\neq\beta\\ \alpha\neq\delta\\ \beta\neq\delta}} \sum_{\substack{a,b\\ c,d}} \langle S_a^\alpha S_b^\beta S_c^\alpha S_d^\delta \rangle_0^2 \tag{C61}$$

and

$$\mathbf{S}_4^b = \frac{1}{2} \sum_{\alpha\neq\beta} \sum_{\substack{a,b\\ c,d}} \langle S_a^\alpha S_b^\beta S_c^\alpha S_d^\beta \rangle_0^2. \tag{C62}$$

Equation (C61) can be reexpressed as

$$\mathbf{S}_4^a = \sum_{\substack{\alpha\neq\beta\\ \alpha\neq\delta\\ \beta\neq\delta}} \sum_{\substack{a,b\\ c,d}} \left(\lambda^{\beta\delta}\delta_{ac}\delta_{bd} + q^{-1}\lambda^{\alpha\beta}\lambda^{\alpha\delta}F_{abcd} + q^{-2}\lambda^{\beta\delta}(\lambda^{\alpha\beta}+\lambda^{\alpha\delta})\sum_{a_1} v_{aca_1}v_{bda_1} \right.$$

$$\left. + \frac{1}{2}q^{-2}(\lambda^{\beta\delta})^2\delta_{ac}\sum_{a_1a_2} v_{ba_1a_2}v_{da_1a_2} + \delta_{ac}\delta_{bd}\sum_{\substack{\eta\neq\alpha\\ \eta\neq\beta\\ \eta\neq\delta}} \lambda^{\beta\eta}\lambda^{\eta\delta} \right)^2, \tag{C63}$$

which gives

$$\mathbf{S}_4^a = -2(q-1)^2\sum_{\beta\neq\delta}(\lambda^{\beta\delta})^2 - 2(q-1)^3\sum_{\beta\neq\delta}(\lambda^{\beta\delta})^3 - 4(q-1)^2\mathrm{Tr}(\lambda^3). \tag{C64}$$

Equation (C62) can be reexpressed as

$$\mathbf{S}_4^b = \frac{1}{2}\sum_{\alpha\neq\beta}\sum_{\substack{a,b\\ c,d}} \left(q^{-2}\lambda^{\alpha\beta}\sum_{a_1} v_{aca_1}v_{bda_1} + \frac{1}{2}q^{-2}(\lambda^{\alpha\beta})^2\sum_{a_1a_2} F_{aca_1a_2}F_{bda_1a_2} \right.$$

$$\left. + \frac{1}{2}(q-1)\delta_{a,c}\delta_{b,d}\left[\sum_{\eta\neq\alpha}(\lambda^{\beta\eta})^2 + \sum_{\eta\neq\beta}(\lambda^{\alpha\eta})^2\right] + q^{-1}\sum_{\substack{\eta\neq\alpha\\ \eta\neq\beta}}\lambda^{\alpha\eta}\lambda^{\eta\beta}\sum_{a_1} v_{aca_1}v_{bda_1} \right)^2, \tag{C65}$$

which gives

$$\mathbf{S}_4^b = \frac{1}{2}(q-1)(q-2)^2\sum_{\alpha\neq\beta}(\lambda^{\alpha\beta})^2 + \frac{1}{2}(q-1)(q-2)^3\sum_{\alpha\neq\beta}(\lambda^{\alpha\beta})^3 + (q-1)(q-2)^2\mathrm{Tr}(\lambda^3). \tag{C66}$$

Finally in Eq. (C46), we only need the nonzero terms of order $O(1)$ and $O(\lambda)$, i.e.,

$$\mathbf{T}_4 = \sum_{\substack{a,b\\ c,d}}\delta_{ac}\delta_{bd}\left[\sum_{\substack{\alpha\neq\beta\\ \alpha\neq\delta\\ \beta\neq\delta}} Q^{\alpha\beta}Q^{\alpha\delta}\lambda^{\beta\delta} + \frac{1}{2}\sum_{\alpha\neq\beta}(Q^{\alpha\beta})^2 + q^{-2}\frac{1}{2}\sum_{\alpha\neq\beta}(Q^{\alpha\beta})^2\lambda^{\alpha\beta}\sum_{a_1} v_{aca_1}v_{bda_1}\right], \tag{C67}$$

which can be reexpressed as

$$\mathbf{T}_4 = (q-1)^2\sum_{\substack{\alpha\neq\beta\\ \alpha\neq\delta\\ \beta\neq\delta}} Q^{\alpha\beta}Q^{\alpha\delta}\lambda^{\beta\delta} + \frac{1}{2}(q-1)^2\sum_{\alpha\neq\beta}(Q^{\alpha\beta})^2.$$

After putting all these results together in Eq. (C21), we find that $-\frac{1}{2}\beta A_2$ is equal to

$$\frac{\beta^4}{8d}N(q-1)\left\{\left[-2(q-1)+\frac{1}{2}(q-2)^2\right]\sum_{\alpha\neq\beta}(\lambda^{\alpha\beta})^2 + \left[-2(q-1)^2+\frac{1}{2}(q-2)^3\right]\sum_{\alpha\neq\beta}(\lambda^{\alpha\beta})^3\right.$$

$$\left. + [-4(q-1)+(q-2)^2]\mathrm{Tr}(\lambda^3) - 2(q-1)\mathrm{Tr}(Q^2\lambda) - (q-1)\sum_{\alpha\neq\beta}(Q^{\alpha\beta})^2\right\}$$

$$+ \frac{\beta^3}{2}\tilde{J}_0N(q-1)(q-2)\left[\sum_{\alpha\neq\beta}(\lambda^{\alpha\beta})^2 + (q-2)\sum_{\alpha\neq\beta}(\lambda^{\alpha\beta})^3 + 2\,\mathrm{Tr}(\lambda^3)\right] + \frac{1}{2}(\beta\tilde{J}_0)^2dN(q-1)\sum_{\alpha\neq\beta}(Q^{\alpha\beta})^2. \tag{C68}$$

The final piece of information that is needed is the relationship between $\lambda^{\alpha\beta}$ and $Q^{\alpha\beta}$. This results from the equation

$$\frac{\partial A_0}{\partial \lambda^{\alpha\beta}} = 0, \tag{C69}$$

which gives

$$Q^{\alpha\beta} = \lambda^{\alpha\beta} + \frac{1}{2}(q-2)(\lambda^{\alpha\beta})^2 + \sum_{\eta} \lambda^{\alpha\eta}\lambda^{\eta\beta}, \tag{C70}$$

$$\lambda^{\alpha\beta} = Q^{\alpha\beta} - \frac{1}{2}(q-2)(Q^{\alpha\beta})^2 - \sum_{\eta} Q^{\alpha\eta}Q^{\eta\beta}, \tag{C71}$$

and

$$(\lambda^{\alpha\beta})^2 = (Q^{\alpha\beta})^2 - (q-2)(Q^{\alpha\beta})^3 - 2Q^{\alpha\beta}\sum_{\eta} Q^{\alpha\eta}Q^{\eta\beta}. \tag{C72}$$

For the second-order term, we therefore have

$$-\frac{1}{2}\beta A_2 = N(q-1)\left\{\sum_{\alpha\neq\beta}(Q^{\alpha\beta})^2\left[\frac{\beta^4}{16d}(q^2-10q+10)\frac{+}{\beta^3}2\tilde{J}_0(q-2)+\frac{1}{2}(\beta\tilde{J}_0)^2 d\right]\right.$$
$$\left. - \sum_{\alpha\neq\beta}(Q^{\alpha\beta})^3\frac{\beta^4}{4d}(q-1) - \mathrm{Tr}(Q^3)\frac{\beta^4}{4d}(q-1)\right\}, \tag{C73}$$

while for the zeroth-order term, we obtain

$$-\beta A_0 = N(p-1)\left[-\frac{1}{4}\sum_{\alpha\neq\beta}(Q^{\alpha\beta})^2 + \frac{1}{12}(q-2)\sum_{\alpha\neq\beta}(Q^{\alpha\beta})^3 + \frac{1}{6}\mathrm{Tr}(Q^3)\right], \tag{C74}$$

and for the first-order term,

$$-\beta A_1 = N(q-1)\frac{\beta^2}{4}\sum_{\alpha\neq\beta}(Q^{\alpha\beta})^2. \tag{C75}$$

After collecting all the pieces together, we finally find (formally setting $\upsilon = 1$)

$$-\beta A \simeq N(q-1)\left[\sum_{\alpha\neq\beta}(Q^{\alpha\beta})^2\left(\frac{\beta^2}{4} - \frac{1}{4} + \frac{\beta^4}{16d}(q^2-10q+10) + \frac{\beta^3}{2}\tilde{J}_0(q-2) + \frac{1}{2}(\beta\tilde{J}_0)^2 d\right)\right.$$
$$\left. + \sum_{\alpha\neq\beta}(Q^{\alpha\beta})^3\left(\frac{1}{12}(q-2) - \frac{\beta^4}{4d}(q-1)\right) + \mathrm{Tr}(Q^3)\left(\frac{1}{6} - \frac{\beta^4}{4d}(q-1)\right)\right]. \tag{C76}$$

APPENDIX D: MEAN-FIELD EQUATIONS FOR THE M-p SPINS MODEL

As in the main text, we focus on the $M = 3$ and $p = 3$ model. In this case, by following the standard procedure described in Ref. 50, one obtains a mean-field solution in terms of the two overlaps $Q^{(1)}$ and $Q^{(2)}$ introduced in the text. Below, we only reproduce the final result. Let us first introduce the notation

$$\nu(\beta, Q^{(1)}, Q^{(2)}, \{S^\alpha\}) = \exp\left[\sum_{\alpha}\beta\sqrt{Q^{(2)}}z_2^\alpha S^\alpha + \sum_{\alpha}\beta\sqrt{\frac{Q^{(1)}}{3}}z_1^\alpha\prod_{\gamma\neq\alpha}S^\gamma\right]. \tag{D1}$$

The self-consistent equations for the two overlaps read

$$Q^{(1)} = \frac{\int\prod_{\alpha=1}^{3}\frac{dz_1^\alpha}{\sqrt{2\pi}}\frac{dz_2^\alpha}{\sqrt{2\pi}}\frac{\{\sum_{\{S\}}\nu(\beta,Q^{(1)},Q^{(2)},\{S^\alpha\})S^1\}^2}{\sum_{\{S\}}\nu(\beta,Q^{(1)},Q^{(2)},\{S^\alpha\})}}{8\exp\left[\beta^2\left(\frac{Q^{(1)}+3Q^{(2)}}{2}\right)\right]}, \tag{D2}$$

$$Q^{(2)} = \frac{\int\prod_{\alpha=1}^{3}\frac{dz_1^\alpha}{\sqrt{2\pi}}\frac{dz_2^\alpha}{\sqrt{2\pi}}\frac{\{\sum_{\{S\}}\nu(\beta,Q^{(1)},Q^{(2)},\{S^\alpha\})S^1S^2\}^2}{\sum_{\{S\}}\nu(\beta,Q^{(1)},Q^{(2)},\{S^\alpha\})}}{8\exp\left[\beta^2\left(\frac{Q^{(1)}+3Q^{(2)}}{2}\right)\right]}. \tag{D3}$$

The free energy [divided by $(m-1)$] is given by

$$F = \frac{3}{2}\beta^2 Q^{(1)} Q^{(2)} + \frac{3}{2}\beta^2 Q^{(2)} + \frac{1}{2}\beta^2 Q^{(1)} + \ln(8) - \frac{\int \prod_{\alpha=1}^{3} \frac{dz_1^\alpha}{\sqrt{2\pi}} \frac{dz_2^\alpha}{\sqrt{2\pi}} \nu \ln \nu(\beta, Q^{(1)}, Q^{(2)}, \{S^\alpha\})}{8 \exp\left[\beta^2 \left(\frac{Q^{(1)}+3Q^{(2)}}{2}\right)\right]}. \tag{D4}$$

APPENDIX E: MEAN-FIELD EQUATIONS FOR THE F MODEL

We assume a 1-RSB ansatz for the matrix $Q^{\alpha\beta}$ and let Q denote the intrastate overlap. The corresponding mean-field equations can be derived by usual methods and read

$$Q = \frac{\int_{-\infty}^{+\infty} \prod_{a=1}^{3} dz_a \frac{e^{-z_a^2/2}}{\sqrt{2\pi}} \frac{\left[\sum_{\mathcal{S}} \mu'(\mathcal{S}) S^1 \exp\left(\beta\sqrt{Q}\sum_a S_a z_a\right)\right]^2}{\sum_{\mathcal{S}} \mu'(\mathcal{S}) \exp\left(\beta\sqrt{Q}\sum_a S_a z_a\right)}}{\sum_{\mathcal{S}} \mu'(\mathcal{S}) \exp\left[\beta^2 \frac{Q}{2} \sum_a (S_a)^2\right]}, \tag{E1}$$

where $\mathcal{S}$ is a short-hand notation for S_1, S_2, S_3 and $\mu'(\mathcal{S}) = \mu(\mathcal{S}) \exp[\beta^2(u - \frac{Q}{2}) \sum_a (S_a)^2]$. The effective field u has to be determined self-consistently from the equation

$$\begin{aligned} u &= \frac{1}{2} \int_{-\infty}^{+\infty} \prod_{a=1}^{3} dz_a \frac{e^{-z_a^2/2}}{\sqrt{2\pi}} \frac{\sum_{\mathcal{S}} \mu'(\mathcal{S}) (S_1)^2 \exp(\beta\sqrt{Q}\sum_a S_a z_a)}{\sum_{\mathcal{S}} \mu'(\mathcal{S}) \exp\left[\beta^2 \frac{Q}{2} \sum_a (S_a)^2\right]} \\ &= \frac{1}{2} \frac{\sum_{\mathcal{S}} \mu(\mathcal{S}) (S_1)^2 \exp[\beta^2 u \sum_a (S_a)^2]}{\sum_{\mathcal{S}} \mu(\mathcal{S}) \exp[\beta^2 u \sum_a (S_a)^2]}. \end{aligned} \tag{E2}$$

By solving numerically these equations, we have obtained the results described in the main text. In the high-temperature, paramagnetic, region regime where $Q = 0$, on-site spin averages can be obtained by just using the measure $\mu'(\mathcal{S})$. In this way, one can compute the correlation functions entering in the expansion of the Gibbs free energy.

*chiara.cammarota@cea.fr
†giulio.biroli@cea.fr
‡tarzia@lptmc.jussieu.fr
§tarjus@lptmc.jussieu.fr

[1] T. R. Kirkpatrick, D. Thirumalai, and P. G. Wolynes, Phys. Rev. A **40**, 1045 (1989).
[2] *Structural Glasses and Super-Cooled Liquids*, edited by P. G. Wolynes and V. Lubchenko (Wiley, 2012).
[3] A. Cavagna, Phys. Rep. **476**, 51 (2009).
[4] C. Cammarota, G. Biroli, M. Tarzia, and G. Tarjus, Phys. Rev. Lett. **106**, 115705 (2011).
[5] C. Brangian, W. Kob, and K. Binder, J. Phys. A **35**, 191 (2002); **36**, 10847 (2003); K. Binder, C. Brangian, and W. Kob, Lecture Notes in Physics Vol. 736 (Springer-Verlag, Berlin, 2008), p. 47.
[6] A. Cruz, L. A. Fernandez, A. Gordillo-Guerrero, M. Guidetti, A. Maiorano, F. Mantovani, E. Marinari, V. Martin-Mayor, A. Munoz Sudupe, D. Navarro, G. Parisi, S. Perez-Gaviro, J. J. Ruiz-Lorenzo, S. F. Schifano, D. Sciretti, A. Tarancon, R. Tripiccione, J. L. Velasco, D. Yllanes, and A. P. Young, Phys. Rev. B **79**, 184408 (2009).
[7] M. P. Eastwood and P. G. Wolynes, Europhys. Lett. **60**, 587 (2002).
[8] E. Marinari, S. Mossa, and G. Parisi, Phys. Rev. B **59**, 8401 (1999).
[9] L. A. Fernandez, A. Maiorano, E. Marinari, V. Martin-Mayor, D. Navarro, D. Sciretti, A. Tarancon, and J. L. Velasco, Phys. Rev. B **77**, 104432 (2008).
[10] F. Krzakal and L. Zdeborova, Phys. Rev. E **76**, 031131 (2007); Europhys. Lett. **81**, 57005 (2008).
[11] J. Yeo and M. A. Moore, Phys. Rev. E **86**, 052501 (2012); Phys. Rev. Lett. **96**, 095701 (2006); M. A. Moore and B. Drossel, *ibid.* **89**, 217202 (2002).
[12] A. J. Bray and M. A. Moore, J. Phys. C **17**, L463 (1984).
[13] D. S. Fisher and D. A. Huse, Phys. Rev. B **38**, 373 (1988); **38**, 386 (1988).
[14] G. Parisi, M. Picco, and F. Ritort, Phys. Rev. E **60**, 58 (1999).
[15] D. J. Gross, I. Kanter, and H. Sompolinsky, Phys. Rev. Lett. **55**, 304 (1984).
[16] F. Caltagirone, G. Parisi, and T. Rizzo, Phys. Rev. E **85**, 051504 (2012).
[17] Since $\pi_{ij}^{-1} = \pi_{ij}$, the interaction $\delta(\sigma_i, \pi_{ij}(\sigma_j))$ is equivalent to $\delta(\pi_{ij}(\sigma_i), \sigma_j)$. Therefore the interaction is symmetric with respect to the exchange of the sites i and j.
[18] Note that the threshold $c_{\rm col}$ for the existence of a coloring transition at $T = 0$ is slightly larger than the limiting RFOT c_K as it is such that[10] $c_{\rm col} \sim 2q \ln(q) - \ln(q) - 1$.
[19] J. Salas and A. Sokal, J. Stat. Phys. **86**, 551 (1997).
[20] On a regular random graph, long-range antiferromagnetic order cannot truly exist. However, one can still calculate the stability of the paramagnetic solution and assign a direction of instability to incipient antiferromagnetism.
[21] A. Georges and J. Yedidia, J. Phys. A. **24**, 2173 (1991).
[22] A. Georges, M. Mézard, and J. Yedidia, Phys. Rev. Lett. **64**, 2937 (1990).
[23] G. Cwilich and T. R. Kirkpatrick, J. Phys. A **22**, 4971 (1989).

[24]F. Caltagirone, U. Ferrari, L. Leuzzi, G. Parisi, and T. Rizzo, Phys. Rev. B **83**, 104202 (2011).
[25]F. Caltagirone, U. Ferrari, L. Leuzzi, G. Parisi, and T. Rizzo (private communication).
[26]C. Cammarota and G. Biroli, Proc. Nat. Acad. Sci. **109**, 8850 (2012).
[27]M. Dzero, J. Schmalian, and P. G. Wolynes, Phys. Rev. B **72**, 100201 (2005); **80**, 024204 (2009).
[28]S. Franz, Europhys. Lett. **73**, 492 (2006); J. Stat. Mech. (2005) P04001.
[29]X. Xia and P. G. Wolynes, Phys. Rev. Lett. **86**, 5526 (2001).
[30]S. Franz, G. Parisi, F. Ricci-Tersenghi, and T. Rizzo, Eur. Phys. J. E **34**, 102 (2011).
[31]C. Cammarota, G. Biroli, M. Tarzia, and G. Tarjus (unpublished).
[32]M. Dzero, J. Schmalian, and P. G. Wolynes, J. Chem. Phys. **129**, 194505 (2008).
[33]J.-P. Bouchaud and G. Biroli, J. Chem. Phys. **121**, 7347 (2004).
[34]A. Cavagna, T. S. Grigera, and P. Verrocchio, Phys. Rev. Lett. **105**, 055703 (2010); G. Biroli, J.-P. Bouchaud, A. Cavagna, T. S. Grigera, and P. Verrocchio, Nat. Phys. **4**, 771 (2008); L. Berthier and W. Kob, Phys. Rev. E **85**, 011102 (2012); F. Sausset and G. Tarjus, Phys. Rev. Lett. **104**, 065701 (2010); G. M. Hocky, T. E. Markland, and D. R. Reichman, *ibid.* **108**, 225506 (2012).
[35]Within replica theory, assuming that the Almeida-Thouless transition line exists, the amplitude of this tail would go to zero at the transition. Within droplet theory, long-range order is destabilized by the field on a length scale ξ_h proportional to $h^{-1/(d/2-\theta)}$, see Ref. 13. The overlap would first decrease toward a value q_1 on length scales of the order of one and then to a value q_0 for cavity sizes larger than ξ_h. However, both close to the remnant of the Almeida-Thouless line and close to $h = 0$ the difference $q_1 - q_0$ is expected to be small. In consequence, the growth of the point-to-set length would only be visible in the tail behavior.
[36]However, one should not conclude that studying disordered fully connected models is always worthless as far as the glass transition is concerned. They may indeed fare better for describing glass-forming liquids than their own finite-dimensional version. This—apparently odd—statement comes from the fact discussed in Sec. VI that models of glass-forming liquids may, after some coarse-graining, behave more as predicted from infinite-dimensional RFOT models than finite-dimensional disordered spin models do. The main advantage then of infinite-dimensional/fully connected models is that they can be rigorously analyzed in depth and that new effects and phenomena can be more easily looked for.
[37]A. Lipowski, J. Phys. A **30**, 7365 (1997).
[38]R. Mari, F. Krzakala, and J. Kurchan, Phys. Rev. Lett. **103**, 025701 (2009).
[39]S. Sasa, Phys. Rev. Lett. **109**, 165702 (2012).
[40]F. Liers, E. Marinari, U. Pagacz, F. Ricci-Tersenghi, and V. Schmitz, J. Stat. Mech. (2010) L05003.
[41]T. Sarlat, A. Billoire, G. Biroli, and J.-P. Bouchaud (unpublished).
[42]G. Biroli and M. Mézard, Phys. Rev. Lett. **88**, 025501 (2002).
[43]M. P. Ciamarra, M. Tarzia, A. de Candia, and A. Coniglio, Phys. Rev. E **67**, 057105 (2003); **68**, 066111 (2003).
[44]R. K. Darst, D. R. Reichman, and G. Biroli, J. Chem. Phys. **132**, 044510 (2010).
[45]S. Karmakar and G. Parisi, Proc. Nat. Acad. Sci. (2013) (to appear).
[46]D. Ruelle, *Thermodynamic Formalism: The Mathematical Structures of Equilibrium Statistical Mechanics*, 2nd ed. (Cambridge University Press, 2004).
[47]R. L. Dobrushin, Theor. Prob. Appl. **13**, 197 (1968).
[48]H. A. Bethe, Proc. R. Soc. London **150**, 552 (1935); R. Peierls, *ibid.* **154**, 207 (1936); L. Onsager, J. Am. Chem. Soc. **58**, 1486 (1936); P. Ro. Weiss, Phys. Rev. **74**, 1493 (1948).
[49]M. Mézard and G. Parisi, Eur. Phys. J. B **20**, 217 (2001).
[50]M. Mézard, G. Parisi, and M. Virasoro, *Spin Glass Theory and Beyond*, Lecture Notes in Physics Vol. 9 (World Scientific, 2004).